Available at www.sciencedirect.com

INFORMATION PROCESSING IN AGRICULTURE xxx (xxxx) xxx

journal homepage: www.elsevier.com/locate/inpa

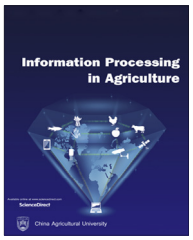

Plant trait estimation and classification studies in plant phenotyping using machine vision – A review

Shrikrishna Kolhar [a,b], *Jayant Jagtap* [c,*]

[a] *Symbiosis International (Deemed University) (SIU), Lavale, Pune, India*
[b] *VPKBIET, Baramati, Maharashtra, India*
[c] *Symbiosis Institute of Technology (SIT), Symbiosis International (Deemed University) (SIU), Lavale, Pune, Maharashtra, India*

ARTICLE INFO

Article history:
Received 1 May 2020
Received in revised form
22 February 2021
Accepted 26 February 2021
Available online xxxx

Keywords:
Plant phenotyping
Machine vision
Plant trait estimation
Imaging techniques
Leaf segmentation and counting
Plant classification studies

ABSTRACT

Today there is a rapid development taking place in phenotyping of plants using non-destructive image based machine vision techniques. Machine vision based plant phenotyping ranges from single plant trait estimation to broad assessment of crop canopy for thousands of plants in the field. Plant phenotyping systems either use single imaging method or integrative approach signifying simultaneous use of some of the imaging techniques like visible red, green and blue (RGB) imaging, thermal imaging, chlorophyll fluorescence imaging (CFIM), hyperspectral imaging, 3-dimensional (3-D) imaging or high resolution volumetric imaging. This paper provides an overview of imaging techniques and their applications in the field of plant phenotyping. This paper presents a comprehensive survey on recent machine vision methods for plant trait estimation and classification. In this paper, information about publicly available datasets is provided for uniform comparison among the state-of-the-art phenotyping methods. This paper also presents future research directions related to the use of deep learning based machine vision algorithms for structural (2-D and 3-D), physiological and temporal trait estimation, and classification studies in plants.

Contents

* Corresponding author.
E-mail address: jayant.jagtap@sitpune.edu.in (J. Jagtap).

https://doi.org/10.1016/j.inpa.2021.02.006

Please cite this article as: S. Kolhar and J. Jagtap, Plant trait estimation and classification studies in plant phenotyping using machine vision – A review, Information Processing in Agriculture, https://doi.org/10.1016/j.inpa.2021.02.006

1. Introduction

Plant phenotyping is a quantitative description of observable traits of plants resulting from the interaction of its genotype, management, and environment (GxMxE). It involves the application of different methods to measure plant traits related to structure, physiology, and temporal events from components (leaf or fruit) to a holistic level (whole plant) [1]. Plant characteristics like chlorophyll content, leaf surface temperature, leaf size, leaf count, shoot biomass, photosynthesis efficiency, plant growth rate, germination time, and emergence time of leaves are measured and analyzed in plant phenotyping studies. Effect of abiotic (such as water deficiency, salinity, nutrient deficiency, and other environmental conditions) and biotic factors (such as microorganisms, insects, parasites, weeds, etc.) on the plant characteristics can be analyzed using plant phenotyping. Nowadays, automatic growth chambers equipped with robotic platforms are used for non-invasive automatic image acquisition of plants for phenotyping [2–5]. Plant phenotyping, in its early days, used red, green, blue (RGB) imaging as primary imaging method for analysis of plant traits related with the plant structure. With advancements in imaging sensors, imaging techniques like hyperspectral imaging, thermal imaging and chlorophyll fluorescence imaging (CFIM), 3-dimensional (3-D) imaging and high resolution volumetric imaging are used for analysis of architectural, temporal, and physiological traits of plants [6,7] [8]. Recently in many of the experiments these imaging techniques are combined for simultaneous analysis of plant traits [9,10]. Humplik et al. [11] gives detailed overview of imaging techniques for non-destructive high-throughput phenotyping of plant shoots. Hamuda et al. [12] presents a comprehensive survey on segmentation techniques based on color index, threshold and learning from previous knowledge. The intent of this paper is to present the review of methodologies based on computer vision, machine learning and deep learning for plant trait estimation and classification problems in plant phenotyping.

To deal with issues of global interest like rapidly growing human population, climate changes, scarce rain falls, soil conditions and various plant diseases, new innovative methodologies need to be designed. These new methods can be used to identify, classify, quantify and predict effects of these factors to enhance production and nutritional value of crop. Therefore, there is need for automatic integrative analysis of plant characteristics to speed up crop variety selections that are better suited for local climatic conditions. Plant phenotyping is also used to study plant diseases. It gives quantitative analysis of pathogen infection on plant physiology. These methods have ability to keep track of physiological functions such as photosynthesis and transpiration, in infected plants. Advanced imaging techniques outside visible light spectrum enable us to identify and quantify disease symptoms that are otherwise not visible by naked eye [13].

A brief overview of imaging techniques and their applications for plant phenotyping are explained in Section 2. Section 3 presents discussion on different stages in image processing approach for plant phenotyping. Section 4 briefly discusses the most recent machine vision approaches considering plant trait estimation and classification problems in the literature reported so far. Section 5 gives information about publicly available datasets and section 6 presents conclusions and future research directions.

2. Imaging techniques overview

2.1. *Digital Color (RGB) imaging*

Digital cameras having high quality charged coupled devices (CCD) with high resolution, dynamic range and sensitivity in the visible light spectrum (400–750 nm), are used for RGB imaging and produce two dimensional images to mimic human vision. The raw image is in the form of spatial matrices of intensity values in the blue (450 nm), green (550 nm) and red (600 nm) spectral bands as shown in Fig. 1. Digital color imaging is used for tracking various parameters related

Please cite this article as: S. Kolhar and J. Jagtap, Plant trait estimation and classification studies in plant phenotyping using machine vision – A review, Information Processing in Agriculture, https://doi.org/10.1016/j.inpa.2021.02.006

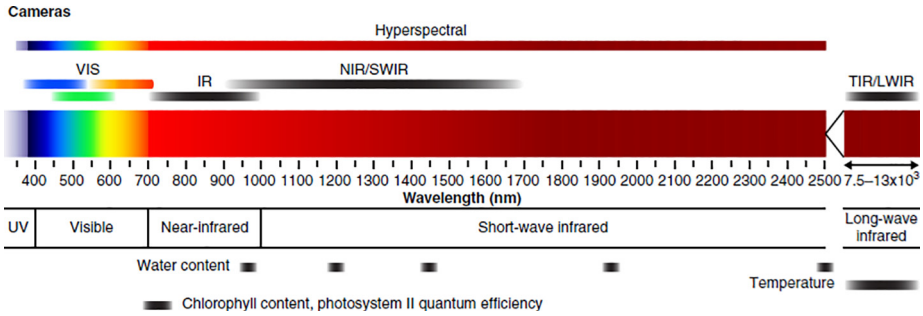

Fig. 1 – Cameras used in plant phenotyping and their wavelengths [9].

to plant growth rate and provides information related to the plant morphology. It enables determination of visible plant characteristics such as shoot biomass, leaf area, leaf count, stem length and count of tillers in non-invasive manner [11,14,15]. Depending on types of crops RGB imaging systems vary. Top view RGB imaging systems are generally used in case of rosette plants for growth rate extraction. RGB top view images of Arabidopsis (Arabidopsis thaliana) and tobacco (Nicotiana tabacum) plants are used to study growth rate under drought stress, chilling stress and biotic stress conditions [16–18]. Plant growth analysis using top view images is affected by overlapping leaves and nastic movement of leaves [18]. This is one of the hurdle when image is captured from one view only (e.g. from top view). The system with multiple views (top view, side views) in RGB imaging solves this problem to certain extent. Multi-view RGB imaging is used, for example, in case of cereals to extract growth rate. Multi-view RGB images of cereals like barley, wheat, rice, sorghum and of pea field cultivars are used to study growth rate under drought stress, salt stress, cold stress and nutrient deficiency [3,11,19]. RGB imaging is low cost and simplest method that increases both speed and accuracy in plant phenotyping. Though visible imaging is most commonly used method, it can only provide structural information of the plants. The factors like overlapping leaves, circadian movement of leaves, similarity in brightness and color between plant and background, canopy shadow and influence of light pose challenges in plant phenotyping using visible imaging and need be addressed using other techniques [7] Table 1.

2.2. *Chlorophyll Fluorescence Imaging (CFIM)*

Chlorophyll fluorescence imaging is used to capture energy emitted by molecules excited at a specific wavelength. CFIM is useful for detecting physiological or pathological defects in plants. Fig. 2 shows the schematic CFIM system. Xenon short-arc lamp is used as a light source. Band pass filter and low pass filter are placed after light source to generate ultraviolet (UV) blue excitation light. Digital light projector generates either uniform or structured illumination. An electron-multiplying CCD camera is used for acquiring fluorescence images. Fluorescence from UV excited green plants is characterized by four wavebands around 440 nm (blue), 520 nm (green), 690 nm (red) and 740 nm (far-red) out of which the last two are due to chlorophyll. Hence, in CFIM, images are captured at these two wavebands. In one of the studies, CFIM system excited with UV-blue light under structured illumination is used for detection of chilling injury in cucumbers [20]. Chlorophyll fluorescence induction (CFIN), the functioning principle of fluorometers, is used for the measurement of chlorophyll fluorescence and provides a great deal of information regarding photosynthetic function [21]. CFIN is used to study plant response to various stresses, as photosynthesis is affected in plants suffering from adverse conditions. Therefore, chlorophyll fluorescence is important parameter for analyzing health of plants [22]. Humplik et al. [23] examined the effect of cold stress on pea field cultivars with multi-view RGB and kinetic type of CFIM (KCFIM) images. Chen et al. [24] studied the effect of drought stress on photosynthetic efficiency of barley plant by excitation of chlorophyll molecules using blue light emitting diode (LED). Jansen et al. [16] analyzed the effect of chilling stress on Arabidopsis photosynthesis efficiency and found that photosynthesis efficiency is significantly reduced under chilling stress condition however it seems to be relatively insensitive for early detection of water stress. Chlorophyll fluorescence imaging is used for early detection of stress symptoms in case of pathogen attack or herbicide treated plants. Most CFIM studies are limited to seedling level of model crops. In the field applications of CFIM power requirement for rapid illumination, robustness, and reproducibility are the areas of improvement.

2.3. *Thermal imaging*

Thermal imaging is used for capturing information in the long wave infrared (LWIR) region (7.5–13 μm) of the electromagnetic spectrum as shown in Fig. 1. Thermal imaging devices consist of optical lens, infrared (IR) sensors/detectors and signal processors to detect thermal/infrared radiations emitted by the object related to its temperature. Lens collects the energy from target object and focuses it on IR sensors/detectors as shown in Fig. 3. An array of IR detectors creates a pattern of temperature called thermogram. This thermogram is first converted into electric pulses and then transformed into thermal image for display. In plant phenotyping, thermal imaging is used to measure plant and leaf surface temperature in non-invasive manner [25]. Plant and leaf surface temperature is an indicative measure of water use efficiency (WUE), transpiration, and leaf stomatal conductance. Plants are cooled using transpiration process by loss of water through leaf stomata. Under drought conditions and salt stress, plant stomata get closed resulting in increased leaf

Please cite this article as: S. Kolhar and J. Jagtap, Plant trait estimation and classification studies in plant phenotyping using machine vision – A review, Information Processing in Agriculture, https://doi.org/10.1016/j.inpa.2021.02.006

Table 1 – Imaging Techniques: Applications, Advantages and Disadvantages.

Imaging Technique	Plant traits	Applications	Advantages	Disadvantages
Digital Color (RGB) Imaging	Structural traits like shoot biomass, leaf area, leaf count. Temoporal traits: plant growth rate, stem angle trajectory, emergence time of leaves	For determination of visible plant characteristics and plant growth analysis	Low cost, simple, fast and accurate	Limited physiological information provided, affected by shadows, changes in ambient light, overlapping leaves and movement of leaves
Chlorophyll Fluorescence Imaging	Physiological triats: Photosynthetic function information, non-photochemical quenching, quantum yield	Assessment of biotic/abiotic stress, effect of disease	Early detection of stress on photosynthesis	Due to small signal to noise ratio difficulties in field, acclimatization required, requirement of high power and data analysis software
Thermal Imaging	Physiological traits: Plant and leaf surface temperature, WUE, leaf stomatal coductance, transpiration	Monitoring of leaf and canopy transpiration rate	Spatial resolution, precise and rapid measurements	Affected by diurnal changes in ambient conditions and soil temperature, extensive calibration and camera angle adjustment required
Hyperspectral Imaging	Physiological traits: Leaf and canopy water content, NDVI, PRI	Assessment of stress, biochemical composition of leaf and canopy	Very promising and reliable method	Frequent camera calibration required, complex data management, expensive hyperspectral cameras
Three Dimensional (3-D) Imaging	Structural traits: Plant height, plant width, root volume, root surface, stem angle. Temporal traits: projected canopy area, stem angle trajectory, emergence time of leaves	Tracking exact geometry of canopy	Used for tracking structural and temporal growth of organs and plants	Complicated data reconstruction for stereo camera systems, for laser scanning instruments specific illumination required
High Resolution Volumetric Imaging (X-ray CT and MRI)	Structural and physiological parameters in 3-D, root length, Water content	Resolving root structure, assessment of severity of disease	MRI detects higher fraction of roots due to strong root to soil contrast, X-ray CT has higher spatial resolution	Ferromagnetic components affect MRI, X-ray effect yet to be investigated on time-series images

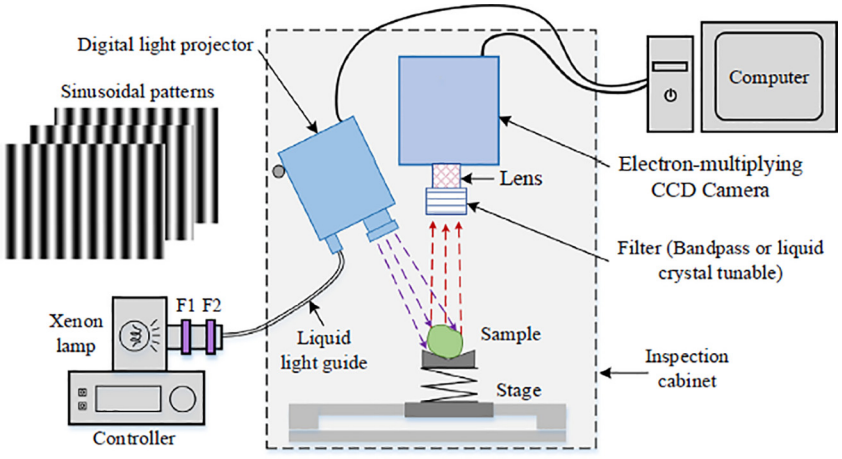

Fig. 2 – Clorophyll fluoroscence imaging setup [20].

Please cite this article as: S. Kolhar and J. Jagtap, Plant trait estimation and classification studies in plant phenotyping using machine vision – A review, Information Processing in Agriculture, https://doi.org/10.1016/j.inpa.2021.02.006

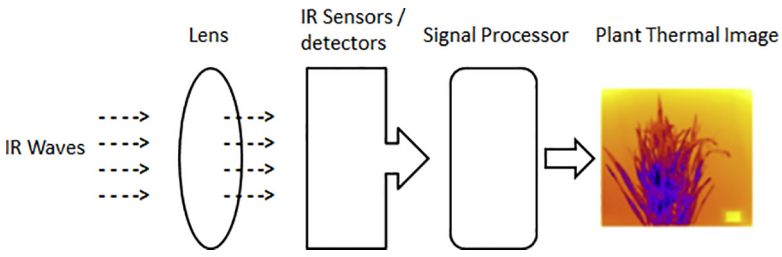

Fig. 3 – Thermal imaging setup.

surface temperature. Water stress index calculated from leaf temperature was used to evaluate and compare stress levels of four different peach trees [26]. Hashimoto et al. [27] analyzed water stress in sunflower leaves using thermal imaging. Jones et al. [28] reported the use of thermal imaging for quantitative analysis of plant behavior to water deficiency in the field. James et al. [29] tested salinity tolerance of wheat seedling using infrared thermal imaging. Siddiqui et al. [30] used thermal imaging for monitoring of rice plant under salt stress. Recently, thermal imaging in combination with RGB imaging is used for monitoring fruit surface temperature to manage apple sunburn [31]. Thermal imaging has several advantages, such as spatial resolution, precise rapid measurements, and monitoring of leaf and canopy transpiration. This makes thermal imaging ideal for comparison of differences in the canopy temperatures. However, thermal imaging is affected by environment and objects around. Furthermore, thermal imaging requires extensive calibration and camera angle adjustment for plants with complex morphology.

2.4. *Hyperspectral imaging*

Hyperspectral imaging operates at the visible, near infrared (NIR) region with spectral range 750–1000 nm and short-wavelength infrared (SWIR) region with spectral range 1000–3000 nm in the electromagnetic spectrum as shown in Fig. 1. Hyperspectral imaging setup consists of hyperspectral camera/spectrograph and halogen lamps as shown in Fig. 4. Halogen lamps are broadband light sources and are commonly used in hyperspectral imaging systems. Reflected light

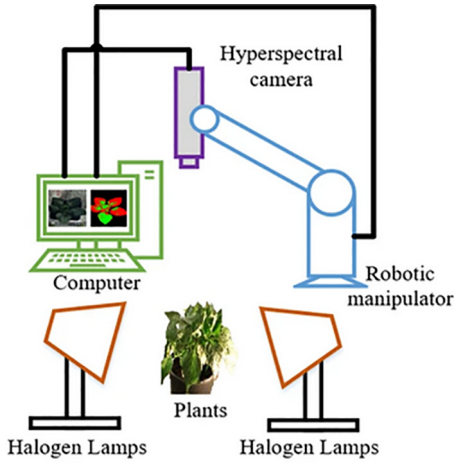

Fig. 4 – Hyperspectral imaging setup [32].

from the object enters through the objective lens and is dispersed into different wavelengths inside the camera. This dispersed light projected onto CCD detectors is converted into electrical signals. Computer interprets the strength of various wavelengths in terms of intensity values. Hyperspectral imaging provides the spectral profile for each pixel in the image. In case of plants, hyperspectral imaging is used for determining the diverse information ranging from water content to leaf pigments such as chlorophyll. Hyperspectral imaging is used for measuring indices such as normalized difference vegetation index (NDVI) an indicator of the chlorophyll content and the photochemical reflectance index (PRI) an indicator of photosynthetic efficiency [11,33]. Harshavardhan et al. [34] analyzed drought tolerance of Arabidopsis plants using hyperspectral NIR imaging and RGB (top-view) imaging. Neilson et al. [35] used hyperspectral NIR imaging and RGB imaging to see response of sorghum plants to nitrogen and water deficiency. Behmann et al. [36] proposed calibration of close-range hyperspectral pushbroom cameras to eliminate the effect of geometrical factors like leaf angle, leaf twisting and self-shading on signals of biological processes. Ge et al. [37] used hyperspectral imaging technique to estimate NDVI. Images at NIR channel (670 nm) and red channel (770 nm) were used to calculate NDVI image: $NDVI = \frac{(NIR_{770nm} - Red_{670nm})}{(NIR_{770nm} + Red_{670nm})}$, which is the most commonly used pair of wavelengths. Seo et al. [38] used the short-wave infrared hyperspectral imaging technique (SWIR-HIT) to detect and classify watermelon seeds infected with the cucumber green mosaic mottle virus (CGMMV). Feng et al. [39] used hyperspectral imaging to monitor the plant traits such as fresh weight, sodium concentration, and photosynthesis related traits of 13 okra (Abelmoschus esculentus L.) genotypes after salt treatment. Applications of hyperspectral imaging for plant phenotyping are very reliable and promising in their infancy. Large volume of data generated using hyperspectral imaging is difficult to handle in high-throughput phenotyping. Relatively expensive hyperspectral cameras restrict their wide adoption in various applications.

2.5. *Three Dimensional (3-D) imaging*

3-D imaging of plants enables tracking exact geometry and measurement of plant growth which is essential for plant phenotyping studies [42]. 3-D imaging helps to differentiate between movement of plants and actual growth on plant and organ level which is otherwise difficult with 2-dimensional (2-D) imaging [43,44]. 3-D imaging techniques are used for measurement of plant traits like plant height,

Please cite this article as: S. Kolhar and J. Jagtap, Plant trait estimation and classification studies in plant phenotyping using machine vision – A review, Information Processing in Agriculture, https://doi.org/10.1016/j.inpa.2021.02.006

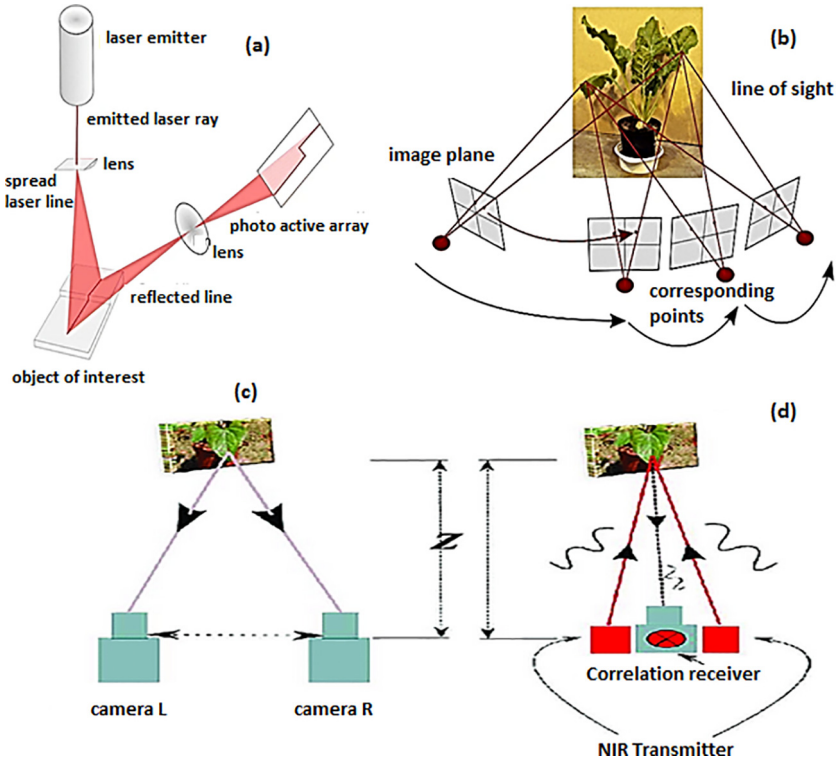

Fig. 5 – 3-D imaging system setup (a) Laser triangulation and (b) Structure from motion [40] (c) Stereo vision and (d) Time-of-flight [41].

plant width, root volume, root surface area, leaf size, leaf width, stem angle and projected canopy area. These plant traits are measured on four different scales such as single plant level, mini plot level, experimental field level and open field level [40]. There are various 3-D measurement techniques like laser triangulation, stereo vision, time-of-flight, structure from motion, structured light approaches and terrestrial laser scanning. Laser triangulation technique involves laser line to illuminate the object of interest and a sensor array to capture laser reflection as shown in Fig. 5(a). As this laser triangulation setup requires low-cost components it is widely used in laboratory experiments [45,46,45]. Recently, laser triangulation approaches with non-visible lasers (700–800 nm) are used in the fields to give better reflection in sunny conditions [47,48]. Structure from motion methods use 2-D RGB images taken by moving camera from multiple angles to reconstruct 3-D models as shown in Fig. 5(b). Parameters like focal length, distortion, position and orientation are estimated for reconstruction of 3-D models [49]. Unlike laser triangulation, structure from motion methods require a single camera and do not need active illumination as they are used on unmanned aerial vehicles (UAVs). In stereo vision system two or more cameras are used to capture two or more images of the scene as shown in Fig. 5 and 3-D scene is recovered from these images. Wu et al. [50] used multi-view stereo 3-D reconstructed images of maize shoots for extraction of phenotypic traits at organ and individual plant level. Structured light setup involves grid or horizontal bars in specific pattern to capture 2-D images and convert them into 3-D information by measuring deformation of the patterns [51]. As these structured light setups are big and require large space they are used in industries. Time-of-flight cameras use time between emitted light and reflected light from thousands of points to construct 3-D image as shown in Fig. 5(d). Due to low resolution, time-of-flight cameras are used in indoor applications [52]. Light field cameras use 2-D image with depth measured from direction of light coming from each pixel on the camera array and estimate 3-D information [53]. Like time-of-flight cameras, light field cameras are also used in indoor applications. Terrestrial laser scanning uses time-of-flight or phase shift approach to scan the environment. 2-D RGB images taken by moving camera are required for reconstruction of 3-D information [54]. Terrestrial laser scanning approaches are mostly used for determining canopy parameters. Big measurable volume and high accuracy are the advantages of terrestrial laser scanning technique. However, the method is time consuming, hard to process and cost intensive.

2.6. *High resolution volumetric imaging*

High resolution techniques like magnetic resonance imaging (MRI) and X-ray computed tomography (CT) as shown in Fig. 6(a and b) are used mainly for phenotyping of roots. MRI applications in plant phenotyping are from imaging of seeds to imaging of fluids [57]. MRI is used for measuring traits like root length, diameter, growth angles and mass. Using MRI, roots of diameter ranging between 200 μm and 300 μm can be measured quantitatively [58]. MRI is used for detecting the symptoms of damage caused by Heterodera schachtii and Rhizoctonia solani on sugar beet [59]. In one of the studies, MRI is used for resolving root structure and separating roots from hetero-specific neighbors for maize

Please cite this article as: S. Kolhar and J. Jagtap, Plant trait estimation and classification studies in plant phenotyping using machine vision – A review, Information Processing in Agriculture, https://doi.org/10.1016/j.inpa.2021.02.006

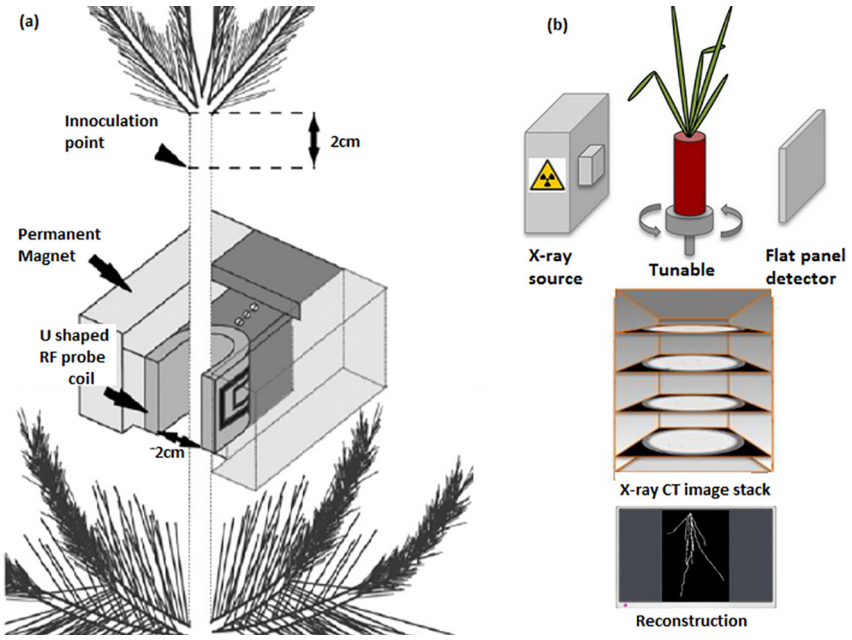

Fig. 6 – High resolution volumetric imaging (a) MRI [55] and (b) X-ray CT [56].

plants [60]. In another study, MRI is used for analyzing the effect of pot size on the growth of barley plants [61]. MRI is used for simultaneous phenotyping of plant shoots and roots. MRI provides temporal information about root growth in petunia cultivars which is not apparent from shoot growth in commercial breeding [62]. X-ray CT imaging is used for measuring volume data of soil and plant structures such as root length [63]. In wheat experiment, root lengths measured using CT images deviate by 8% [64]. Gargiulo et al. [65] used X-ray micro CT scanning for quinoa (Chenopodium quinoa Willd) seed phenotyping to measure parameters such as embryo volume and weight ratios which showed positive correlation with protein content. Hughes et al. [66] used X-ray micro CT images of wheat plants for measurement of spike and grain morphometric parameters. Adaptive threshold and morphology algorithm were used to analyze spike and grain growth of wheat plants exposed to high temperatures under two different water treatments to investigate specific root details and finely graduated root diameters of thin roots. Soltaninejad et al. [67] used multi-resolution encoder-decoder networks for volumetric segmentation of wheat roots using CT images. Still, MRI and X-ray CT for 3-D root imaging pose different opportunities and challenges. X-ray CT provides higher spatial resolution whereas MRI detects higher fractions of the roots than CT as MRI provides strong root-to-soil contrast [68].

3. Image pre-processing and segmentation

Image processing and computer vision methods are widely used for detecting plant traits and identifying proper genotype in the given environment. Fig. 7 shows commonly used steps in plant phenotying using 2-D image processing. This section presents two important steps in plant phenotyping i.e. image pre-processing and segmentation.

3.1. *Pre-processing*

Pre-processing is the processing of the raw images captured by a camera which includes contrast enhancement and noise filtering. Image can be enhanced by adjusting the contrast of an image to overcome luminance issues. Low pass filter is applied on image to remove high frequency noise. Homomorphic filter is used to overcome illumination issues for the plant images captured in the fields [69]. Image cropping is another pre-processing step used to extract image containing the target objects from the entire image [70]. Data augmentation is also a pre-processing step used to increase variation in image datasets to make algorithms more robust [71].

3.2. *Segmentation*

In the processing of RGB plant images the main task is to separate the plant from the background. After the plant is separated from background, next task is to segment plant leaves to determine plant growth and leaf count [69,71]. Various segmentation methods used for plant phenotyping can be classified as: color index, threshold and learning-based segmentation [12]. Table 2 lists the types of segmentation techniques, methodologies adopted, and their advantages and disadvantages.

3.2.1. *Color index-based segmentation*

In computer vision, color index-based segmentation is the most common method used for segmenting the plant from the background. RGB color space is converted into other color space with green indices such as normalized difference index (NDI): $128 \times \left[\frac{(G-R)}{(G+R)} + 1\right]$, excess green index (ExG): $(2 \times G - R - B)$, where R, G and B are red, green and blue components, respectively. Ge et al. [37] used color index-based segmentation in which the image was transformed to single

Please cite this article as: S. Kolhar and J. Jagtap, Plant trait estimation and classification studies in plant phenotyping using machine vision – A review, Information Processing in Agriculture, https://doi.org/10.1016/j.inpa.2021.02.006

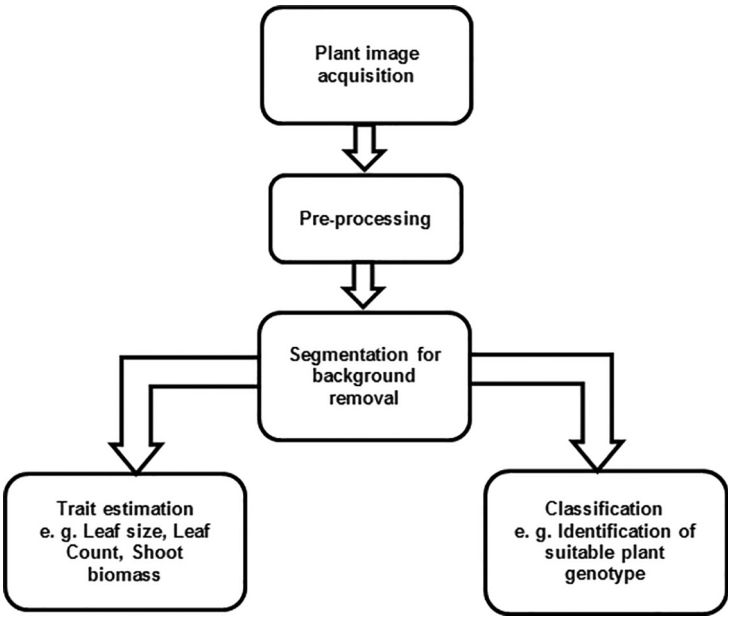

Fig. 7 – Image processing steps in plant phenotyping.

Table 2 – Comparison of Segmentation Techniques.

Type of Segmentation	Methods	Advantages	Disadvantages
Color-index based segmentation	NDI, ExG, excess green minus excess red index (ExGR), colour index of vegetation extraction (CIVE), vegetative index (VEG), modified excess green index, combined ExG, CIVE, and VEG indices [78–81,37,73]	Easy to compute, widely used, showed good adaptability in outdoor environment	Do not perform well when the light is high or low, poor adaptability with shadow
Threshold-based segmentation	Dynamic threshold, hysteresis threshold, entropy of a histogram, Otsu threshold, homogeneity threshold, automatic threshold [82–88,33,74]	Good in handling gradual light changes, automatic method, fairly simple	More computation time, threshold adjustments required in extreme light conditions
Learning-based segmentation	Environmentally adaptive segmentation algorithm, mean-shift algorithm with back propagation neural network, support vector machines, decision tree based segmentation model, particle swarm optimization clustering and morphology modeling [75,89,90,72,77,91,71]	Robust to illumination variations, deals with shadow and reflected regions	Long run time and dependency on training data

color-band image using the formula $\frac{2\times G}{(B+R)}$. Guerrero et al. [72] used a support vector machine (SVM), and a combination of ExG, color index of vegetation extraction (CIVE), and vegetative index for automatic plant discrimination in maize fields impregnated by soil materials. Choudhury et al. [73] used color based segmentation in hue, saturation and value (HSV) color space for a holistic and components based phenotyping of maize plants. Color index-based segmentation techniques are easy to implement but perform poorly in changing illumination conditions [12].

3.2.2. *Threshold-based segmentation*

Choosing correct threshold is vital in segmentation of images. High threshold may lead to under-segmentation and low

Please cite this article as: S. Kolhar and J. Jagtap, Plant trait estimation and classification studies in plant phenotyping using machine vision – A review, Information Processing in Agriculture, https://doi.org/10.1016/j.inpa.2021.02.006

threshold may cause over-segmentation. There are various techniques used for selection of proper threshold. Some of these techniques are dynamic thresholding, hysteresis thresholding, entropy of a histogram, homogeneity threshold and Otsu's adaptive thresholding. Bai et al. [33] used Otsu's adaptive thresholding for the segmentation of plant from background. Lima et al. [74] used automatic histogram segmentation for the extraction of plants in different soil conditions. Threshold-based segmentation techniques require more computation time as large number of iterations are required for choosing proper threshold level [12].

3.2.3. *Learning-based segmentation*

As color index-based segmentation techniques fail to perform well in extreme illumination conditions, machine learning (supervised and unsupervised) based approaches with color indices were used to distinguish between plant pixels and background. For example, Meyer et al. [75] used an unsupervised machine learning method named fuzzy clustering to extract plant pixels from the excess green and excess red images. Zheng et al. [76] reported a supervised mean-shift algorithm and back propagation neural network to segment the plant from background. To address the illumination problems such as shadow, Guo et al. [77] used a learning-based decision tree method to separate the plant pixels from non-plant pixels. Mochida et al. [71] presented a review of machine learning approaches used for the semantic and instance segmentation. Learning-based thresholding requires long run time and its performance relies on the training data [12].

4. Trait estimation and classification studies

Plant phenotyping involves the application of computer vision, machine learning, and deep learning algorithms for obtaining useful biological information. This section presents recent advancements in the area of plant phenotyping related to the plant trait estimation and classification studies.

4.1. *2-D trait estimation studies*

Plant trait estimation is one of the important problems in machine vision. The studies related to structural (Table 3), physiological (Table 4) and temporal trait (Table 5) estimation are discussed in the following sub-sections.

4.1.1. *Structural traits*

In the early days, image processing and computer vision algorithms were used for non-invasive automatic phenotyping of plants. In one of the studies, Pape et al. [92] estimated a 3-D color histogram to separate foreground from background in plant images. Euclidean distance vector based method was used for finding center points of plant leaves and split lines of overlapping leaves. Region growing algorithm was used for leaf counting. The method was applied on Arabidopsis and tobacco plant RGB images taken from the leaf segmentation challenge (LSC) dataset [93,94]. The leaf segmentation for tobacco was comparatively poor than that of Arabidopsis. This was indicated by the best-dice coefficient (which indicates the quality of individual leaf segmentation) of 53% for tobacco and 77% for Arabidopsis plant. Bai et al. [33] used color images to determine green pixel fraction (GPF), an indicator of vegetation biomass. RGB images were first transformed into $L^\star a^\star b^\star$ color space where color is expressed as three values: $L^\star$ indicates brightness from black (0) to white (100), $a^\star$ ranges from green (−) to red (+), and $b^\star$ ranges from blue (−) to yellow (+). Then, Otsu's adaptive thresholding was used for segmentation of plants. It was observed that from Jun/30 to Jul/8, GPF showed fast plant growth. But, during Jul/8 to Aug/10, GPF was almost constant and average GPF was between 0.53 and 0.58. Because of full canopy and soybean turned yellow after maturation, half of the pixels were misclassified as background and a drop was observed in the value of GPF. Ge et al. [37] used two side view RGB imaging to determine the plant projected area (PA) correlated with leaf area (LA), plant shoot fresh weight (FW) and dry weight (DW). Easy to compute color index-based segmentation was used for separating plant from background and morphological opening was used to remove isolated noise. Correlation of plant projected area with leaf area and fresh weight was greater than 0.98 whereas 0.952 with dry weight. Wang et al. [95] applied Chan-Vese model and sobel operator for segmentation of overlapping crop leaves. A color feature having hues with high levels of green was used to segment plant leaves from the background. Chan-Vese model and sobel operators were used to extract leaf contours and detect leaf edges, respectively. Then, the results were combined to extract target leaf from the complex background and to determine overlapping of leaves. By using this segmentation method, the mean error rate and standard deviation were reduced to 0.0428 ± 0.0230. Praveen Kumar et al. [15] first converted the RGB image into hue, saturation and value (HSV) image and used v-plane of brightness to enhance the image. Skewness of v-plane brightness distribution was used to reduce excessive brightness and shadow effect on leaves. Then the leaf region was extracted from the background using graph based technique. Circular Hough transform (CHT) was used for leaf counting. This method achieved leaf segmentation accuracy of 95.4%. Leaf counting accuracy expressed in terms of the difference in leaf count (DiC) and the absolute difference in leaf count ($|DiC|$) were (−) 0.7 and 2.30, respectively. Machine learning for feature extraction needs image processing and analysis [96]. Minervini et al. [97] used color information ($a^\star$ and $b^\star$ components in $L^\star a^\star b^\star$ color space) and texture features to distinguish between plant and background. Gaussian mixture model (GMM) is used to extract arbitrary complex shaped plant leaves from the surrounding. This method performs well for images with complex and changing background and achieved the segmentation accuracy of 96.44% in terms of dice similarity coefficient. Al-Vshakarji et al. [98] used 2-D RGB images of rosette plants taken from LSC dataset [93,94]. In this work, k-means and expectation maximization (EM) algorithm were used for plant extraction from the background. Distance map transform, watershed segmentation and stem linking algorithm were used for the tracking of plant leaves. The segmentation accuracy of 74.4% and foreground-background separation dice coefficient of 0.94 were obtained using this approach. Bodner et al. [99] used hyperspectral imaging for plant root phenotyping. Unsupervised techniques including multi-level thresholding, k-means clustering, fuzzy clustering

Please cite this article as: S. Kolhar and J. Jagtap, Plant trait estimation and classification studies in plant phenotyping using machine vision – A review, Information Processing in Agriculture, https://doi.org/10.1016/j.inpa.2021.02.006

Table 3 – Structural Trait Estimation Studies.

Study	Plant Trait	Methodology	Results	Plant Species	Dataset
			Computer Vision Approaches		
Pape et al. [92]	Leaf size, leaf count	3-D histograms, Euclidean distance map and region growing method	Dice 53% for tobacco and 77% for Arabidopsis	Arabidopsis, tobacco	Public LSC [93,94]
Bai et al. [33]	Plant height and vegetation biomass	RGB to $L^\star a^\star b^\star$ conversion, Otsu's adaptive thresholding	GPF range 0.53–0.58	Soybean, wheat	Private [33]
Ge et al. [37]	Plant PA, LA, FW, DW	Color index-based segmentation	Correlation PA with LA and FW 0.98, and with DW 0.952	Soybean and wheat plants	Private [37]
Wang et al. [95]	Leaf size	Chan-Vese model and Sobel operator	Mean error and standard deviation 0.0428 ± 0.0230	Cucumber plant	Private [95], Public [112]
Praveen Kumar et al. [15]	Leaf size, leaf count	RGB to HSV conversion, graph based technique and CHT	Segmentation accuracy 95.4%, DiC −0.7, $\lvert DiC \rvert$ 2.3	Arabidopsis and tobacco plant	Public LSC [93,94]
			Machine Learning Approaches		
Minervini et al. [97]	Canopy area, Leaf area, leafcount	Color, texture features and Gaussian Mixture Model (GMM)	Dice 96.44%	Arabidopsis plant	Public LSC [93,94]
Al-Vshakarji et al. [98]	Canopy area, Leaf area, leaf count	Distance map transform, Watershed segmentation and stem linking algorithm	Segmentation accuracy 74.4%, dice 0.94	Arabidopsis, tobacco plant	Public LSC [93,94]
Bodner et al. [99]	Root length, root regions and root decay	Multi-level thresholding, k-means clustering, fuzzy clustering and SVM	Segmentation accuracy for Subsoil 49% and for topsoil 84.1%	Wheat plant root	Private [99]
Jiang et al. [100]	Leaf count	Google Inception Net V3, Fisher Vector (FV), RF	MSE 0.32	Maize plant	Private [100]
Falk et al. [101]	Root shape, length, mass and angle	k-means and Convolutional auto-encoder segmentation	F1-score 0.8824, IOU 0.8725	Soybean plant roots	Private [101]
			Deep Learning Approaches		
Aich et al. [103]	Leaf size, leaf count	Deep de-convolution and convolution	DiC 0.73, $\lvert DiC \rvert$ 1.62	Arabidopsis, tobacco plant	Public LSC [93,94]
Pound et al. [104]	Spike and spikelet count	CNN with four stacked hourglass network	Counting accuracy 95.91% for spikes and 99.66% for spikelets	Wheat plant	Public ACID [104]
Salvador et al. [105]	Leaf size, Leaf count	RNN	Dice 74.7%, DiC 1.10	Arabidopsis, tobacco plant	Public LSC [93,94]
Dobrescu et al. [106]	Leaf size, leaf count	Modified ResNet50	DiC 0.19, MSE 1.56	Arabidopsis, tobacco plant	Public LSC [93,94], ImageNet [107]
Ubbens et al. [14]	Leaf size, count	CNN	$\lvert DiC \rvert$ 0.48, MSE 0.73	Arabidopsis, tobacco plant	Public LSC[93,94], Private [14]
Morris et al. [108]	Leaves detection	Pyramid CNN and watershed segmentation	Average precision 0.96, dice 0.952	Trees, vines and bushes	Private [108]
Liu et al. [109]	Maize tassel count	Faster R-CNN with ResNet and VGGNet	Average precision ResNet 94.99%, VGGNet 91.51%	Maize plant	Private [113]
Praveen Kumar et al. [110]	Leaf size, leaf count	Orthogonal transform coefficients, CNN models AlexNet and VGG19	Dice 94.7, DiC 0.11, $\lvert DiC \rvert$ 0.03	Arabidopsis, tobacco plant	Public LSC [93,94]
Lin and Guo [111]	Panicle count	U-Net	Accuracy 95.5 % and RMSE 2.5	Sorghum plants	Private [111]

Please cite this article as: S. Kolhar and J. Jagtap, Plant trait estimation and classification studies in plant phenotyping using machine vision – A review, Information Processing in Agriculture, https://doi.org/10.1016/j.inpa.2021.02.006

Table 4 – Physiological Trait Estimation Studies.

Study	Plant Trait	Methodology	Results	Imaging Method	Plant Species	Dataset
Ge et al. [37]	WUE and LWC	NDVI	Mean LWC 80.1%, R^2 0.92, RPD 3.78	Hyperspectral imaging	Soybean and wheat plants	Private [37]
Bai et al. [33]	Plant temperature, Vegetation indices	NDVI	R^2 with NDVI-SRS and NDVI-spec 0.49–0.65 and for RE-NDVI 0.46–0.68	Thermal, hyperspectral and RGB imaging	soybean and wheat	Private [33]
Pandey et al. [114]	Water content, chemical macro and micro-neutrients	NDVI, PCA, PSLR	Leaf water content R^2 0.93 and RPD 3.8, macro-nutrients R^2 = 0.69–0.92 and RPD = 1.62–3.62	Hyperspectral imaging	Maize and soybean plants	Private [114]
Misra et al. [115]	NIR-MGI, leaf FW	Background subtraction, Otsu's thresholding, Sobel operator, ANN	RMSE 0.13 and MAPE 9.65	Visual-NIR imaging	Rice plants	Private [115]
Lima et al. [74]	Vegetation indices, morphological traits	Automatic histogram segmentation, connected components, shape parameters and vegetative indices	Segmentation accuracy 92%	Multi-spectral imaging	Tomato plants	Private [74]
Rehman et al. [116]	Relative water content	CNN with modified inception module	R^2 0.872	Visible near infrared hyperspectral imaging	Maize plants	Private [116]

Table 5 – Temporal Trait Estimation Studies.

Study	Plant Trait	Methodology	Results	Imaging Method	Plant Species	Dataset
Dellen et al. [18]	Plant growth signatures	Canny edge detector, Leaf shape model and graph based linking algorithm	Accuracy 96%	Infrared imaging	Tobacco plant	Private [18]
Choudhury et al. [117]	Stem angle	Color based segmentation, fast marching distance transform, time-series clustering	Accuracy 84%	Multiview RGB imaging	Five panicoid grain crops	Public panicoid phenomap-1 [117]
Agarwal [118]	Plant emergence detection	Hierarchical adaptive segmentation based on Chan-Vese active contour, heat map based optical flow detector	Emergence time under 10 h	High dynamic range images	Maize and foxtail millet	Private[118]
Das Choudhury et al. [73]	Leaf length, skeleton area, apex curvature	Graph based approach, fast marching distance transform	Accuracy for UNL-CPPD-I and II are 92 and 85%.	Multiview RGB imaging	Maize plants	Public UNL-CPPD-I and II [117]
Jiang et al. [119]	Count of emerging blooms, flowering patterns	Faster RCNN	R^2 0.88 and RMSE 0.79	Multiview RGB imaging	Cotton plants	Private [119]

Please cite this article as: S. Kolhar and J. Jagtap, Plant trait estimation and classification studies in plant phenotyping using machine vision – A review, Information Processing in Agriculture, https://doi.org/10.1016/j.inpa.2021.02.006

and supervised technique such as two class support vector machine (SVM) were used for segmentation of roots. In topsoil, segmentation accuracy was high in comparison with the subsoil. In the subsoil segmentation accuracy was 49% as thresholding failed in 78.6%, of the cases. In the topsoil, segmentation accuracy was 84.1% of all the cases and SVM being the best with accuracy of 90%. Jiang et al. [100] used multi-scale Google Inception Net V3 architecture for leaf feature extraction and Fisher Vector to reduce redundant information. These reduced feature maps along with random forest (RF) algorithm are used for prediction of leaf counts. The proposed method achieves mean square error (MSE) of 0.32 and |DiC| of 0.35. However, abnormal illumination and leaf occlusions introduce large errors in leaf counting. Falk et al. [101] used k-means and convolutional auto-encoder architecture for segmentation of soybean roots and studied various traits like root shape, length, mass and angle. Root segmentation using this method resulted in F1-score and intersection over union (IOU) of 0.8824 and 0.8725, respectively.

Deep learning algorithms have performed well on a wide range of plant phenotyping tasks, such as plant identification and classification, leaf segmentation and counting, and root localization [102]. Aich et al. [103] used a deconvolution network for plant extraction from the background and a convolutional network for counting leaves. Semantic segmentation is done using convolutional sub-network consisting of multiple convolutional layers, pooling and normalization operations followed by deconvolutional sub-network consisting of convolution transpose, un-pooling and normalization. This method is capable of identifying leaf shapes in overlapping conditions. This method achieved DiC of 0.73 and |DiC| of 1.62. Pound et al. [104] presented annotated crop image dataset (ACID) and used deep learning method namely convolutional neural network (CNN) based on stacked hourglass network for accurately localizing wheat spikes and spikelet. Input RGB image of size 256 × 256 is reduced to 64 × 64 by initial residual blocks, Hourglass network generated output heat-map of size 64 × 64 pixels with one for every feature. Mean squared error (MSE) loss function was used for training. Non-maximal suppression (NMS) algorithm was used to detect position of spikes and spikelets from each heat-map. This network achieves counting accuracy of 95.91% for spikes and 99.66% for spikelets. Salvador et al. [105] applied recurrent neural network (RNN) for semantic instance segmentation on LSC dataset [93,94]. Segmentation accuracy obtained in terms of symmetric best dice was 74.7% and DiC was 1.10 indicating leaf counting accuracy. Dobrescu et al. [106] treated leaf counting problem as direct regression problem instead of instance segmentation. In this study, modified Resnet50 deep residual network pre-trained on ImageNet dataset [107] was used for leaf counting. The study proposed that using multiple plant datasets even with different cultivars for training, improves the performance of deep neural network. Results of leaf counting were improved at least by 50% in terms of MSE and |DiC| using multiple datasets. The model learns more precise features due to increased data variability. Ubbens et al. [14] used deep learning for leaf counting of rosette plants and demonstrated that use of 3-D synthetic plants to augment dataset mitigates the problem of dataset shift while training and testing on different datasets. Ara2013-Canon dataset [93,94] was augmented with synthetic rosettes to form a training set. 27% reduction in mean absolute count error (|DiC|) was observed using this training set. Training and testing of the model on real datasets (Ara2012 and Ara2013-Canon) resulted in degradation of performance due to dataset shift. However, training on purely synthetic dataset mitigates the dataset shift with mean count error (|DiC|) centered more around zero. Morris et al. [108] presented a Dense-Leaves dataset and used pyramid CNN algorithm and watershed segmentation for detection of leaf boundaries. Average precision in predicting the leaf boundary pixels was observed to be 0.96 and the dice score was 0.952 indicating segmentation accuracy. This method needs to be tested on leaves with weak boundary cues. Since Dense-Leaves dataset has 108 images only, it is challenging to enable training of deeper models. Liu et al. [109] used faster region based CNN (R-CNN) with ResNet and VGGNet for counting maize tassels in RGB images taken using unmanned aerial vehicle (UAV). Average precision of 94.99% was obtained using ResNet101 and was the best model for maize tassel detection as compared to VGGNet. Praveen Kumar et al. [110] used orthogonal transform coefficients for plant region segmentation and deep CNN models AlexNet and VGG19 leaf counting. Segmentation accuracy achieved in terms of foreground background dice score was 94.7% and leaf counting accuracy in terms of DiC and |DiC| was 0.11 and 1.03, respectively. In another study, Lin and Guo [111] used U-Net CNN model for segmentation and counting of Sorghum panicles. An accuracy of 95.5% and root mean square error (RMSE) of 2.5 is achieved in this study and it ensures accurate yield estimation and enhanced Sorghum breeding efficiency.

4.1.2. *Physiological traits*

In one of the studies, Ge et al. [37] used hyperspectral imaging techniques to analyze WUE and leaf water content (LWC). In case of hyperspectral imaging, images at NIR channel (670 nm) and red channel (770 nm) were used to calculate NDVI image: $NDVI = \frac{(NIR_{770nm} - Red_{670nm})}{(NIR_{770nm} + Red_{670nm})}$. NDVI image was used to extract plant from non-plant pixels. Then leaf reflectance spectra was obtained for prediction of LWC. Mean LWC was 80.1% obtained from 44 sample plant images. Hyperspectral imaging predicted LWC satisfactorily with correlation for determination of R^2 0.92 and ratio of performance to deviation (RPD) of 3.78. RPD greater than 3 indicates that the developed model is good or analytical quality model. Bai et al. [33] used multi-sensor system consisting of thermal infrared radiometer, NDVI sensor, portable spectrometer and digital color camera integrated on a single platform. Plant height, temperature and NDVI by NDVI sensor were recorded directly without preprocessing. NDVI-SRS (NDVI measured by the NDVI sensor) and NDVI-spec (NDVI measured by the portable spectrometers) exhibited the same patterns whereas RE-NDVI-spec (red-edge NDVI measured by the portable spectrometers) exhibited the same pattern as other two but had a lower amplitude. Correlation of grain yield with NDVI-SRS and NDVI-spec was between 0.49 to 0.65 and for RE-NDVI between 0.46 to 0.68. Pandey et al. [114] used hyperspectral imaging to analyze effect of water and nutrient stress on maize and soy-

Please cite this article as: S. Kolhar and J. Jagtap, Plant trait estimation and classification studies in plant phenotyping using machine vision – A review, Information Processing in Agriculture, https://doi.org/10.1016/j.inpa.2021.02.006

bean plants. First raw image data was converted into 3-D image cubes and then red (705 nm) and NIR (750 nm) channel images were used to extract NDVI image as $NDVI = \frac{(NIR_{750nm} - Red_{705nm})}{(NIR_{750nm} + Red_{705nm})}$. This NDVI image was used to extract plant pixels from all image bands along the wavelength giving average reflectance and spectral data. Principal component analysis (PCA) was used to remove outliers in spectral data and partial least squares regression (PLSR) was used to determine water content, macro and micro-nutrient concentration. Among all leaf water content had highest accuracy given by R^2 of 0.93 and RPD of 3.8. All macro-nutrients also quantified satisfactorily with R^2 from 0.69 to 0.92 and RPD from 1.62 to 3.62. Misra et al. [115] calculated green leaf proportion (GLP) from visible images and mean gray intensity (MGI) from NIR images. GLP and NIR-MGI were input to artificial neural network (ANN) to estimate leaf fresh weight (FW). RMSE and mean absolute percentage error (MAPE) between predicted and ground truth leaf FW were 0.13 and 9.65, respectively. This approach outperforms conventional approach based on projected shoot area. Lima et al. [74] used automatic histogram segmentation, connected components, shape parameters and vegetative indices for analyzing fertilization strategy for tomato plants using multi-spectral imaging. NDVI image was used for extraction of plant from background. Automatic histogram segmentation algorithm achieved 92% accuracy in segmentation of NDVI image. In one of the studies, Rehman et al. [116] used CNN with a modified inception module to predict the relative water content of maize plants from top view images captured using visible near infrared hyperspectral camera. The proposed method achieved R^2 of 0.872 which outperformed the other two standard methods namely partial least square regression and SVM regression.

4.1.3. *Temporal traits*

Due to constant variations in plant architecture, extracting meaningful traits from temporal phenotyping remains critical challenge. Dellen et al. [18] investigated the growth of tobacco plants using time-lapse videos of growing plants. Canny edge detector was used to determine edge map of the images. These edges were split into contour segments. Leaf shape model was used to group contour segments for leaf detection. To deal with problems like leaf movement and leaf growth a graph-based tracking algorithm was used to link leaf detection in neighboring image frames. Leaf tracking performance was 96% for default image size and the performance slightly decreased after down-sizing of the images. In one of the studies, Das Choudhury et al. [117] used stem angle for temporal plant phenotyping of five panicoid grain crops: maize, sorghum, pearl millet, proso millet and foxtail millet. Stem angle computation involves segmentation, view selection, skeletonization and stem angle measurement. Frame differencing and color based segmentation were used for extracting plant from the background. Fast marching distance transform was used for skeletonization. A time-series clustering analysis was performed to determine temporal patterns of the stem angles. Cluster purity analysis further provides necessary insights into genetics of the plants. Stem angle computation accuracy of 84% was obtained using this approach. Higher purity value for a particular genotype indicates more homogeneity between plants. Agarwal [118] introduced an automatic method for plant emergence detection. Color based segmentation was used for separating plant from background soil. Then hierarchical adaptive segmentation based on Chan-Vese active contour was used for segmentation and tracking of plant. Heat map based optical flow approach was used for detection of movement of soil as an early indication of plant emergence. The method was tested on a dataset consisting of 76 plants and plant images were captured at 5 min interval. The emergence was observed in 40 plants. For 95% of the plants, predicted time of emergence was under 10 h and for 75% of the plants was under 4 h of the ground truth. Das Choudhury et al. [73] used graph based approach to determine component phenotypes such as leaf length, integral leaf-skeleton area, mid-leaf curvature, apex curvature and stem angle. These phenotypes were obtained from the sequence of images of maize plants and demonstrated genetic influence on the temporal variations of these phenotypes. The method was tested on University of NebraskaLincoln component plant phenotyping dataset I and II (UNL-CPPD-I and II). Average plant level accuracy in in terms of leaf detection was 92% for UNL-CPPD-I and 85% for UNL-CPPD-II, respectively. In another study, Lin and Guo [119] used faster region based CNN (RCNN) model for detection and counting of emerging blooms of individual cotton plants to determine flowering curves over the flowering time. R^2 of 0.88 and RMSE of 0.79 showed that the method is effective in detection and counting of emerging blooms of cotton plants.

4.2. *3-D trait estimation studies*

Vandenberghe et al. [120] and Paulus et al. [40] presented a review on 3-D image acquisition, processing and trait analysis. Table 6 provides the details of 3-D trait estimation studies. Aksoy et al. [121] presented a novel multi-level procedure for finding and tracking leaf growth of rosette plants using infrared stereo image sequences. Background was removed using thresholding and depth map was computed from pair of stereo images using block matching technique. Superparamagnetic clustering method was used for segmentation of leaves followed by segment merging using leaf-shape descriptor to recover leaves represented by more than one segment. Root-mean-square (RMS) error between actual and estimated number of leaves was 1.0021 using superparamagnetic clustering and found to be less than that of graph-based method. He et al. [122] used 3-D imaging for phenotyping of strawberry plants in which point cloud segmentation and orienting bounding box using eigenvector of co-variance matrix and clustering algorithm based on Euclidean distance were employed to derive strawberry color, height, width, length, calyx size and achene number. Concordance correlation coefficient (CCC) was used to calculate concordance between ground truth and 3-D fruit traits. Best concordance CCC greater than 0.9 and correlation R^2 greater than 0.9 were found for fruit dimensions and volume. For calyx size, CCC equal to 0.86 and R^2 equal to 0.87 were obtained indicating weaker concordance. For achene number, CCC equal to 0.67 and R^2 equal to 0.77 were obtained indicating weak concor-

Please cite this article as: S. Kolhar and J. Jagtap, Plant trait estimation and classification studies in plant phenotyping using machine vision – A review, Information Processing in Agriculture, https://doi.org/10.1016/j.inpa.2021.02.006

Table 6 – 3-D Trait Estimation Studies.

Study	Plant Trait	Methodology	Results	Imaging Method	Plant Species	Dataset
Aksoy et al. [121]	Plant growth signatures, Leaf size, leaf count	Super-paramagnetic clustering, leaf shape model	RMS error 1.0021	Infrared 3-D Stereo imaging	Tobacco plants	Private [121]
He et al. [122] Private [122]	Strawberry color, height, width, volume, calyx size and achene number	Point cloud segmentation, Orienting bounding box, eigenvector of co-variance matrix, Clustering based on Euclidean distance	For fruit dimension and volume	CCC $> 0.9, R^2 > 0.9$, for calyx size CCC = 0.86, $R^2 = 0.87$, for achene size CCC = 0.67, $R^2 = 0.77$	3-D imaging	Strawberry plants
Bernotas et al. [123]	Leaf size, count, 3-D plant growth, diel leaf hyponastic movement	End-to-end RNN and R-CNN	For R-CNN SBD = 0.814 and FBD = 0.946, for RNN SBD = 0.560 and FBD = 0.891	Photometric stereo-based 3-D imaging system	Arabidopsis plant	Public PS-plant [123]
Van Dusschoten et al. [58]	Root length, growth angles, number of tips and root mass	Thresholding, dilation and Dijkstra's algorithm	Root mass 70 to 80%, root length 80%	MRI imaging	Barley and maize plants	Private [58]
Hu et al. [124]	Twenty-two 3-D traits like Grain number, grain shape, grain size and grain density	Otsu's algorithm, watershed segmentation based on the Euclidean distance, PCA	MAPE 2.41% and 4.65%, R^2 0.960 and 0.980	X-ray CT imaging	Rice plant	Private [124]
Choudhury et al. [125]	Volume of onvex hull, stem, TLC and individual leaves, total number of plant voxels, stem cross-section area	3-D voxel-grid reconstruction, voxel overlapping consistency check and point cloud clustering	3.5 min for 3-D voxel grid reconstruction	Muli-view RGB imaging	Maize and cotton plants	Public [125]

Please cite this article as: S. Kolhar and J. Jagtap, Plant trait estimation and classification studies in plant phenotyping using machine vision – A review, Information Processing in Agriculture, https://doi.org/10.1016/j.inpa.2021.02.006

dance. Bernotas et al. [123] used end-to-end RNN and mask R-CNN for instance segmentation of rosette RGB images recorded using photometric stereo 3-D plant phenotyping platform. Best results were obtained using R-CNN with symmetric best dice (SBD) ranging from 0.806 to 0.814 for leaf segmentation and foreground-background dice (FBD) ranging from 0.940 to 0.946 for rosette segmentation. In comparison, RNN performance was poor with SBD ranging from 0.440 to 0.560 for leaf segmentation and FBD ranging from 0.798 to 0.891 for rosette segmentation. High resolution volumetric imaging techniques are also used to obtain 3-D traits. In one of the studies, MRI imaging was used for extraction of quantitative traits from 3-D high quality images of root systems [58]. Thresholding, dilation and Dijkstra's algorithm were used to obtain morphological skeleton of the root system. Dijkstra's algorithm was used to connect each voxel to the base of the root. In this study, root traits such as root length, growth angles, number of tips and root mass were determined from 3-D MRI images of barley and maize plants. This method detected 70 to 80% of root mass and 80% of the total root length using MRI imaging. Recently, Hu et al. [124] used X-ray CT to obtain twenty-two 3-D rice grain traits. Otsu's global adaptive algorithm was used for grain segmentation. Watershed segmentation based on the Euclidean distance transform was used for separating overlapping grains. PCA was used for extraction of grain size. Grain volume was calculated by counting number of voxels in the connected region. Mean absolute percentage error (MAPE) for grain length and grain number were 2.41% and 4.65%, respectively. R^2 values for grain length and grain number were 0.960 and 0.980, respectively. In addition, grain volume, grain number, and total surface area and the total grain weight were correlated with value of R^2 greater than 0.94. In one of the studies, Choudhury et al. [125] presented an algorithm to compute 3-D plant phenotypes using voxel-grid reconstruction from multi-view images of maize and cotton plants. 3-D phenotypes like the volume of convex-hull, total number of plant voxels, stem cross-section area, volumes of the stem, top leaf cluster (TLC), and individual leaves are computed using voxel overlapping consistency and point cloud clustering techniques.

4.3. *Classification studies in plant phenotyping*

As machine learning and deep learning techniques are used for data-driven predictions and classifications, they are playing important role in image based plant phenotyping [71]. Table 7 provides details of the classification studies in plant phenotyping. Lee et al. [126] used visual geometry group 16 (VGG16) network to develop plant identification system from plant organs for LifeClef 2016 plant classification task [127]. Classification accuracy of 61.7% was obtained by training VGG16 on PlantClef2015 dataset from scratch. Whereas pretrained VGG16 on ImageNet data gives an accuracy of 71.2% with an improvement of 9.5%. Without data-augmentation classification accuracy obtained was 56.4% whereas after data augmentation accuracy was 71.2% with an improvement of 14.8%. Lottes et al. [128] used random forest classifier for classification of sugar beet and weeds using keypoint-based and object-based features. For keypoint-based classification, the true positive rate (TPR) for sugar beet was 98% with a precision of 95% and for object-based classification TPR was 94% with a precision of 90%. For the combined approach, TPR was 99% with precision of 95%. Lee et al. [129] used CNN and deconvolutional neural network to learn leaf features for plant classification. Malyakew leaf dataset consisting of 44 plant leaf classes was used in this experiment. The classification accuracy was 98.1% using leaf features learned from CNN. Guo et al. [130] used machine learning methods namely random forest (RF), neural network (NN) and support vector machine (SVM) for the determination of plant root water status based on visible and NIR imaging. Total 37 traits categorized as morphological traits (19), color traits (6) and NIR (12) traits were extracted from each plant image. Classification accuracy is analyzed at different times of the day, in different weather conditions and for different cultivars. For all the three models (RF, NN, SVM), mean prediction accuracy was greater than 90% and Cohen's kappa coefficient was higher than 0.85. Pound et al. [104] in first classification problem used CNN to predict if wheat root tip is present or not given a root system image and in second problem tried to identify if it is leaf tip, leaf base, ear tip or ear base if image of plant shoot is given. This method achieved an accuracy of 98.4% for root tip detection and 97.3% for shoot part classification. Taghavi Namin et al. [131] used CNN and long short-term memories (LSTMs) for the classification of Arabidopsis thaliana plant into its accessions Sf-2, Cvi, Landsberg (Ler-1) and Columbia (Col-0). CNN was used to learn features automatically for classifier. LSTMs were used to learn temporal information such as growth and dynamic behavior of plants. This temporal information was used as discriminating phenotype for plant genotype classification. This method provided classification accuracy of 93%. Beikmohammadi et al. [132] applied MobileNet CNN architecture on two datasets namely Flavia [133] with 32 classes and Leafsnap [134] with 184 classes for classification of plants based on leaf characteristics. This method achieved classification accuracy of 99.6% and 90.54% with Flavia and Leafsnap databases, respectively. Moghimi et al. [135] used six feature selection methods: correlation-based feature selection, reliefF, sequential feature selection, support vector machine-recursive feature elimination (SVM-RFE), least absolute shrinkage and selection operator (LASSO) logistic regression, and RF feature selection. Quadratic discriminant analysis (QDA) classifier was used for classifying the salt-treated vegetation pixels from the control pixels. This ensemble feature selection method reduced hyperspectral features from 215 to 15 spectral features. While spectral features were reduced, the classification accuracy was improved by 8.5% from 68.49% to 77.09%. Lee et al. [70] used simple linear iterative clustering (SLIC) algorithm for feature extraction in $L^{\star}a^{\star}b^{\star}$ color space and compared performance of three classifiers namely SVM, RF and multilayer perceptron (MLP) for plant growth analysis. For the validation dataset, average F1-scores were 92.24, 91.67 and 91.56% for RF, SVM and MLP, respectively. For the test dataset, F1-scores were dropped to 84.60, 76.90 and 76.60% for RF, SVM and MLP, respectively. Venal et al. [136] used hybrid model in which CNN was used for feature extraction and SVM for clas-

Please cite this article as: S. Kolhar and J. Jagtap, Plant trait estimation and classification studies in plant phenotyping using machine vision – A review, Information Processing in Agriculture, https://doi.org/10.1016/j.inpa.2021.02.006

Table 7 – Classification Studies in Plant Phenotyping.

Study	Methodology	Results	Imaging Method	Class Information	Dataset
Lee et al. [126]	VGG16 CNN architecture	Accuracy 71.2%	RGB imaging	Based on 7 organs identify plant images of 1000 species	Public LifeClef [127]
Lottes et al. [128]	Statistical and shape features and RF classifier	TPR 99% with 95% precision	RGB and NIR imaging	Sugar beet and weeds	Private [128]
Lee et al. [129]	CNN and deconvolutional neural network	Accuracy 98.1%	RGB images	44 Plant leaf classes	Private [129]
Guo et al. [130]	RF, NN and SVM	Mean accuracy 90% and Cohen's kappa coefficient 0.85	RGB and NIR imaging	Pakchoi plants root zone water status	Private [130]
Pound et al. [104]	Convolutional neural network (CNN)	Root tip detection accuracy 98.4% and shoot part classification accuracy 97.3%	RGB imaging	Wheat plant: root tip, root negative and leaf tip, leaf base, ear tip, ear base, shoot negative	Private [104]
Taghavi Namin et al. [131]	CNN and LSTM	Accuracy 93%	RGB imaging	Arabidopsis thaliana: Sf-2, Cvi, Landsberg (Ler-1) and Columbia (Col-0)	Public Deep Phenotyping [131]
Beik-mohammadi et al. [132]	MobileNet CNN	Accuracy of 99.6% for Flavia dataset and 90.54% for Leafsnap dataset	RGB imaging	Flavia dataset with 32 classes and Leafsnap dataset with 184 classes	Public Flavia [133], Leaf-snap [134]
Moghimi et al. [135]	Correlation-based, ReliefF, sequential, SVM-RFE, LASSO logistic regression, RF and QDA	Accuracy 77.09%	Hyper-spectral imaging	Salt-stressed wheat plants and healthy plants	Private [135]
Lee et al.[70]	RGB to Lab conversion, SLIC feature extraction and SVM, RF and MLP classifiers	F1 - scores for RF 84.6%, SVM 76.9% and MLP 76.6%	RGB imaging	Rosette plant	Private [70]
Venal et al. [136]	CNN as feature extractor and SVM	Accuracy 97.11%	RGB imaging	Biotic (e.g., fungal and bacterial) and abiotic (e.g., nutrient deficiency and chemical injury) stresses	Private [140]
Pacifico et al. [137]	DT, KNN, weighted KNN, RF and MLP	Accuracy for RF and MLP-BP above 97%, KNN 61.68% and weighted KNN 89.56%	RGB imaging	15 medicinal plants	Private [137]
Fuentes-Pacheco et al. [138]	SegNet CNN	Accuracy 93.84%	RGB imaging	Fig. plant images into crop and background	Private [138]
Anami et al. [139]	SFFS for feature selection and BPNN, SVM, and k-NN for stress classification	Classification accuracy of 89.12% for BPNN, 84.44% for SVM and 76.34 % for k-NN	RGB imaging	Paddy crop varieties: Jaya, Abhilasha, Mugad Suganda, Mugad101, and Mugad Siri	Private [139]

Please cite this article as: S. Kolhar and J. Jagtap, Plant trait estimation and classification studies in plant phenotyping using machine vision – A review, Information Processing in Agriculture, https://doi.org/10.1016/j.inpa.2021.02.006

sification of biotic and abiotic stresses on soybean leaf images. This method achieved classification accuracy of 97.11%. Pacifico et al. [137] used color and texture features along with five classifiers decision tree (DT), k-nearest neighbors (KNN), weighted KNN, RF and multi-layered perceptron with back propagation (MLP-BP) for classification of medicinal plants. Classification accuracy for RF and MLP-BP classifiers was above 97% while it was 94.4% for DT. Whereas accuracies of 61.68% and 89.56% were obtained using KNN and weighted KNN, respectively. Fuentes-Pacheco et al. [138] used SegNet CNN architecture for the segmentation and classification of Fig. plant RGB images into crop and non-crop part. Even with the complex background and variable visual appearance, this method achieved an accuracy of 93.84%. Anami et al. [139] developed a system for paddy crop stress identification and classification. In this work, lower order color moments and visual color descriptors are used as features to examine two biotic and eleven abiotic stresses on five paddy crop varieties. The sequential forward floating selection (SFFS) algorithm is used for feature selection and back propagation neural network (BPNN), SVM and k-NN are used for differentiating between different stresses among which BPNN achieved highest average stress classification accuracy of 89.12 %. Based on the results obtained in the studies so far, the performance of deep learning models is better than the other methods in terms of their plant segmentation accuracy, leaf counting accuracy, classification accuracy, localization wheat spikes, spikelets, and plant roots. However, availability of only few public datasets with small number of sample images for training restricts the training of deep neural networks.

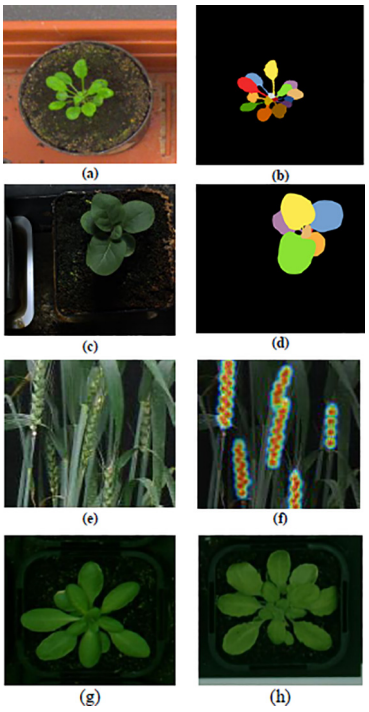

Fig. 8 – Sample plant images (a) Arabidopsis plant RGB image, (b) Labeled leaf image for Arabidopsis plant, (c) Tobacco plant RGB image (d) Labeled leaf image for tobacco plant [93], (e) Wheat plant image, (f) Wheat spikelets [104], (g) and (h) RGB top view images of Arabidopsis thaliana accessions Ler-1 and Cvi respectively [131].

5. Publicly available datasets

Recent advancements in computational tools and quality of sensors, benefited the plant science and engineering community with the availability of public datasets for plant phenotyping. Plant focused computer vision challenges encouraged this community to work on the common datasets. The importance of publicly available datasets is that performance of different methods can be tested on the same dataset. Standard datasets help to improve biological insights into the experimental results and facilitates the analysis of statistical and meta-data [141]. Scharr, H. et al. [93,97] presented with annotated dataset of top view color images of rosette plants. Dataset consists of two types of plant images: one with various cultivars of Arabidopsis plant and another with tobacco undergoing different treatments. The dataset helps for the advancements in leaf segmentation and counting algorithms designed for rosette plants. Pound et al. [104] has presented a dataset called annotated crop image dataset (ACID), with accurately labeled wheat plant images. Dataset contains 520 images of wheat plants for detection and counting of spikes and spikelets. Lobet et al. [142] presents image analysis database having total 28 datasets with 18,13,806 images which are categorized by plant organs and species. Taghavi Namin et al. [131] presented a dataset which includes top-view images of 4 different varieties of Arabidopsis thaliana. 22 top-view images of each plant were taken on consecutive days. This dataset is released for segmentation, growth tracking and accession classification. Cruz et al. [143] presented a multi-modality plant image database comprising of two subsets for Arabidopsis and bean plants. This dataset uses four different image capture modalities including fluorescence, RGB color, depth and infrared. This dataset has 2160 Arabidopsis and 325 bean plant images in above four modalities. Uchiyama et al. [144] presented two datasets for 3-D plant phenotyping: multiview dataset containing plant images captured with three cameras and RGB-D dataset containing both RGB and depth images of plants captured with RGB-D camera. Bernotas et al. [123] presented a photometric stereo dataset with annotated leaf masks to determine advanced traits like 3-D growth of rosette plants and nastic leaf movement. Choudhury et al. [117] presented panicoid phenomap-1, UNL-CPPD and UNL-3DPPD image datasets consisting of RGB images of 40 genotypes of five panicoid grain crops namely maize, sorghum, pearl millet, proso millet, and foxtail millet. These datasets are released to encourage determination of a holistic and components based phenotypes. All these datasets motivate and encourage computer vision community to develop algorithms for plant phenotyping. Sample plant images from some of these datasets are shown in Fig. 8.

Please cite this article as: S. Kolhar and J. Jagtap, Plant trait estimation and classification studies in plant phenotyping using machine vision – A review, Information Processing in Agriculture, https://doi.org/10.1016/j.inpa.2021.02.006

6. Conclusion and future research direction

In this paper, various imaging techniques used in plant phenotyping are assessed based on their applications, advantages and limitations. Digital color imaging is useful for determination of structural plant traits whereas CFIM, thermal imaging and hyperspectral imaging for physiological traits. MRI and X-ray CT imaging is used for phenotyping of plant roots. Imaging techniques outside visible band are also used to quantify disease symptoms which is otherwise not possible by visible RGB imaging. 3-D imaging is used for determination a holistic and component phenotypes. Temporal traits like plant growth patterns, germination time, emergence of leaves and reproductive organs can be measured by using time series images of plants. In this review, color-based segmentation, threshold-based segmentation and learning based segmentation methods are compared along with their applications. Color index-based methods though commonly used for plant phenotyping suffer from shadow and high light variations. Threshold-based segmentation methods work well in changing light conditions but require more computation time as several steps are required to adjust the threshold. Learning based approaches have high accuracy but are complex as several training steps are required for accurate segmentation. This paper also reviews the recent machine vision methods used for plant phenotyping ranging from simple image processing algorithms to complex deep neural networks. A brief overview of plant trait estimation and classification studies is provided in terms of imaging techniques used, plant traits measured, plant species treated, datasets used, and results obtained, for the uniform comparison among state-of-the-art methods and future research advancements. Major challenges in plant phenotyping are light conditions, complex background, overlapping leaves and circadian movement of plant leaves which motivate researchers to develop more sophisticated and accurate machine vision algorithms for plant phenotyping. Temporal information about plants i.e. timing information about events e.g. time of germination, emergence of leaves and senescence of leaves can be used to extract information about plant growth rate and to analyze effect of stresses on plants. Investigation of phenotypes for identification of plant species robust to specific type of stress and categorization of amount of stress on plants are the challenges in plant phenotyping. Advanced 3-D phenotype estimation algorithms need to be developed for accurate characterization of plants. Machine learning and deep learning being data-driven approaches, can be used for early detection of stress before the appearance of visual symptoms. Deep learning approaches can be used along with imaging techniques like hyperspectral imaging and 3-D imaging as they comprise of large number of sample images.

Declaration of Competing Interest

The authors declare that they have no known competing financial interests or personal relationships that could have appeared to influence the work reported in this paper.

REFERENCES

[1] Choudhury SD, Samal A, Awada T. Leveraging image analysis for high-throughput plant phenotyping. Frontiers. Plant Sci 2019;10.
[2] Araus JL, Cairns JE. Field high-throughput phenotyping: the new crop breeding frontier. Trends Plant Sci 2014;19(1):52–61.
[3] Golzarian MR, Frick RA, Rajendran K, Berger B, Roy S, Tester M, et al. Accurate inference of shoot biomass from high-throughput images of cereal plants. Plant Methods 2011;7(1):2.
[4] Jansen M, Pinto F, Nagel KA, van Dusschoten D, Fiorani F, Rascher U, et al. Non-invasive phenotyping methodologies enable the accurate characterization of growth and performance of shoots and roots. In: Genom Plant Genet Resour. Netherlands: Springer; 2013. p. 173–206.
[5] Pieruschka R, Schurr U. Plant phenotyping: Past, present, and future. Plant Phenomics 2019;2019:1–6.
[6] Fiorani F, Schurr U. Future scenarios for plant phenotyping. Annu Rev Plant Biol 2013;64(1):267–91.
[7] Li L, Zhang Q, Huang D. A review of imaging techniques for plant phenotyping. Sensors 2014;14(11):20078–111.
[8] Roitsch T, Cabrera-Bosquet L, Fournier A, Ghamkhar K, Jiménez-Berni J, Pinto F, et al. Review: New sensors and data-driven approaches—a path to next generation phenomics. Plant Sci 2019;282:2–10.
[9] Fahlgren N, Gehan MA, Baxter I. Lights, camera, action: high-throughput plant phenotyping is ready for a close-up. Curr Opin Plant Biol 2015;24:93–9.
[10] Walter A, Liebisch F, Hund A. Plant phenotyping: from bean weighing to image analysis. Plant Methods 2015;11(1):14.
[11] Humplík JF, Lazár D, Husičková A, Spíchal L. Automated phenotyping of plant shoots using imaging methods for analysis of plant stress responses – a review. Plant Methods 2015;11(1).
[12] Hamuda E, Glavin M, Jones E. A survey of image processing techniques for plant extraction and segmentation in the field. Comput Electron Agric 2016;125:184–99.
[13] Mutka A, Bart R. Image-based phenotyping of plant disease symptoms. Front Plant Sci 2014;5:734.
[14] Ubbens J, Cieslak M, Prusinkiewicz P, Stavness I. The use of plant models in deep learning: an application to leaf counting in rosette plants. Plant Methods 2018;14(1).
[15] Kumar JP, Domnic S. Image based leaf segmentation and counting in rosette plants. Inform Process Agric 2019;6 (2):233–46.
[16] Jansen M, Gilmer F, Biskup B, Nagel KA, Rascher U, Fischbach A, et al. Simultaneous phenotyping of leaf growth and chlorophyll fluorescence via GROWSCREEN FLUORO allows detection of stress tolerance in arabidopsis thaliana and other rosette plants. Funct Plant Biol 2009;36(11):902.
[17] Clauw P, Coppens F, Beuf KD, Dhondt S, Daele TV, Maleux K, et al. Leaf responses to mild drought stress in natural variants of arabidopsis. Plant Physiol 2015;167(3):800–16.
[18] Dellen B, Scharr H, Torras C. Growth signatures of rosette plants from time-lapse video. IEEE/ACM Trans Comput Biol Bioinf 2015;12(6):1470–8.
[19] Hairmansis A, Berger B, Tester M, Roy SJ. Image-based phenotyping for non-destructive screening of different salinity tolerance traits in rice. Rice 2014;7(1).
[20] Lu Y, Lu R. Enhancing chlorophyll fluorescence imaging under structured illumination with automatic vignetting correction for detection of chilling injury in cucumbers. Comput Electron Agric 2020;168:105145.
[21] Lazár D. Parameters of photosynthetic energy partitioning. J Plant Physiol 2015;175:131–47.

Please cite this article as: S. Kolhar and J. Jagtap, Plant trait estimation and classification studies in plant phenotyping using machine vision – A review, Information Processing in Agriculture, https://doi.org/10.1016/j.inpa.2021.02.006

[22] Bresson J, Vasseur F, Dauzat M, Labadie M, Varoquaux F, Touraine B, et al. Interact to survive: Phyllobacterium brassicacearum improves arabidopsis tolerance to severe water deficit and growth recovery. PLoS ONE 2014;9(9): e107607.
[23] Humplík JF, Lazár D, Fürst T, Husičková A, Hýbl M, Spíchal L. Automated integrative high-throughput phenotyping of plant shoots: a case study of the cold-tolerance of pea (pisum sativum l.). Plant Methods 2015;11(1):20.
[24] Chen D, Neumann K, Friedel S, Kilian B, Chen M, Altmann T, et al. Dissecting the phenotypic components of crop plant growth and drought responses based on high-throughput image analysis. Plant Cell 2014;26(12):4636–55.
[25] Fehér-Juhász E, Majer P, Sass L, Lantos C, Csiszár J, Turóczy Z, et al. Phenotyping shows improved physiological traits and seed yield of transgenic wheat plants expressing the alfalfa aldose reductase under permanent drought stress. Acta Physiologiae Plantarum 2013;36(3):663–73.
[26] yeong Lee A, Kim SY, Hong SJ, hyeok Han Y, Choi Y, Kim M, et al. Phenotypic analysis of fruit crops water stress using infrared thermal imaging. J Biosyst Eng 2019;44(2):87–94.
[27] Hashimoto Y, Ino T, Kramer PJ, Naylor AW, Strain BR. Dynamic analysis of water stress of sunflower leaves by means of a thermal image processing system. Plant Physiol 1984;76(1):266–9.
[28] Jones HG, Serraj R, Loveys BR, Xiong L, Wheaton A, Price AH. Thermal infrared imaging of crop canopies for the remote diagnosis and quantification of plant responses to water stress in the field. Funct Plant Biol 2009;36(11):978.
[29] James RA, Sirault XRR. Infrared thermography in plant phenotyping for salinity tolerance. In: Plant Salt Tolerance. Humana Press; 2012. p. 173–89.
[30] Siddiqui ZS, Cho JI, Park SH, Kwon TR, Lee GS, Jeong MJ, et al. Phenotyping of rice in salt stress environment using high-throughput infrared imaging. Acta Botanica Croatica 2014;73(1):312–21.
[31] Shi G, Ranjan R, Khot LR. Robust image processing algorithm for computational resource limited smart apple sunburn sensing system. Inform Process Agric 2020;7 (2):212–22.
[32] Wang D, Vinson R, Holmes M, Seibel G, Bechar A, Nof S, et al. Early detection of tomato spotted wilt virus by hyperspectral imaging and outlier removal auxiliary classifier generative adversarial nets (OR-AC-GAN). Sci Rep 2019;9(1).
[33] Bai G, Ge Y, Hussain W, Baenziger PS, Graef G. A multi-sensor system for high throughput field phenotyping in soybean and wheat breeding. Comput Electron Agric 2016;128:181–92.
[34] Harshavardhan VT, Son LV, Seiler C, Junker A, Weigelt-Fischer K, Klukas C, et al. AtRD22 and AtUSPL1, members of the plant-specific BURP domain family involved in arabidopsis thaliana drought tolerance. PLoS ONE 2014;9 (10):e110065.
[35] Neilson EH, Edwards AM, Blomstedt CK, Berger B, Møller BL, Gleadow RM. Utilization of a high-throughput shoot imaging system to examine the dynamic phenotypic responses of a c4 cereal crop plant to nitrogen and water deficiency over time. J Exp Bot 2015;66(7):1817–32.
[36] Behmann J, Mahlein AK, Paulus S, Kuhlmann H, Oerke EC, Plümer L. Calibration of hyperspectral close-range pushbroom cameras for plant phenotyping. ISPRS J Photogramm Remote Sens 2015;106:172–82.
[37] Ge Y, Bai G, Stoerger V, Schnable JC. Temporal dynamics of maize plant growth, water use, and leaf water content using automated high throughput RGB and hyperspectral imaging. Comput Electron Agric 2016;127:625–32.
[38] Seo Y, Lee H, Bae HJ, Park E, Lim HS, Kim MS, et al. Optimized multivariate analysis for the discrimination of cucumber green mosaic mottle virus-infected watermelon seeds based on spectral imaging. J Biosyst Eng 2019;44(2):95–102.
[39] Feng X, Zhan Y, Wang Q, Yang X, Yu C, Wang H, et al. Hyperspectral imaging combined with machine learning as a tool to obtain high-throughput plant salt-stress phenotyping. Plant J 2019;101(6):1448–61.
[40] Paulus S. Measuring crops in 3d: using geometry for plant phenotyping. Plant Methods 2019;15(1).
[41] Kazmi W, Foix S, Alenyà G, Andersen HJ. Indoor and outdoor depth imaging of leaves with time-of-flight and stereo vision sensors: Analysis and comparison. ISPRS J Photogramm Remote Sens 2014;88:128–46.
[42] Ziamtsov I, Navlakha S. Plant 3d (p3d): a plant phenotyping toolkit for 3d point clouds. Bioinformatics 2020;36 (12):3949–50.
[43] Dornbusch T, Lorrain S, Kuznetsov D, Fortier A, Liechti R, Xenarios I, et al. Measuring the diurnal pattern of leaf hyponasty and growth in arabidopsis - a novel phenotyping approach using laser scanning. Funct Plant Biol 2012;39 (11):860.
[44] Lou L, Liu Y, Shen M, Han J, Corke F, Doonan JH. Estimation of branch angle from 3d point cloud of plants. In: 2015 International Conference on 3D Vision. IEEE; 2015. p. 554–61.
[45] Dupuis J, Kuhlmann H. High-precision surface inspection: Uncertainty evaluation within an accuracy range of 15μm with triangulation-based laser line scanners. J Appl Geodesy 2014;8(2).
[46] Paulus S, Dupuis J, Riedel S, Kuhlmann H. Automated analysis of barley organs using 3d laser scanning: An approach for high throughput phenotyping. Sensors 2014;14 (7):12670–86.
[47] Kjaer K, Ottosen CO. 3d laser triangulation for plant phenotyping in challenging environments. Sensors 2015;15 (6):13533–47.
[48] Virlet N, Sabermanesh K, Sadeghi-Tehran P, Hawkesford MJ. Field scanalyzer: An automated robotic field phenotyping platform for detailed crop monitoring. Funct Plant Biol 2017;44(1):143.
[49] Rose J, Paulus S, Kuhlmann H. Accuracy analysis of a multi-view stereo approach for phenotyping of tomato plants at the organ level. Sensors 2015;15(5):9651–65.
[50] Wu S, Wen W, Wang Y, Fan J, Wang C, Gou W, et al. MVS-pheno: A portable and low-cost phenotyping platform for maize shoots using multiview stereo 3d reconstruction. Plant Phenomics 2020;2020:1–17.
[51] Zhang S. High-speed 3d shape measurement with structured light methods: A review. Opt Lasers Eng 2018;106:119–31.
[52] Corti A, Giancola S, Mainetti G, Sala R. A metrological characterization of the kinect v2 time-of-flight camera. Robot Autonom Syst 2016;75:584–94.
[53] Polder G, Hofstee J. Phenotyping large tomato plants in the greenhouse using a 3d light-field camera. American Society of Agricultural and Biological Engineers Annual International Meeting 2014, ASABE 2014;2014(1):153–9.
[54] Vezočnik R, Ambrožič T, Sterle O, Bilban G, Pfeifer N, Stopar B. Use of terrestrial laser scanning technology for long term high precision deformation monitoring. Sensors 2009;9 (12):9873–95.
[55] Umebayashi T, Fukuda K, Haishi T, Sotooka R, Zuhair S, Otsuki K. The developmental process of xylem embolisms in pine wilt disease monitored by multipoint imaging using compact magnetic resonance imaging. Plant Physiol 2011;156(2):943–51.
[56] Rogers ED, Monaenkova D, Mijar M, Nori A, Goldman DI, Benfey PN. X-ray computed tomography reveals the response of root system architecture to soil texture. Plant Physiol 2016;171(3):2028–40.

Please cite this article as: S. Kolhar and J. Jagtap, Plant trait estimation and classification studies in plant phenotyping using machine vision – A review, Information Processing in Agriculture, https://doi.org/10.1016/j.inpa.2021.02.006

[57] Borisjuk L, Rolletschek H, Neuberger T. Surveying the plant's world by magnetic resonance imaging. Plant J 2012;70 (1):129–46.
[58] van Dusschoten D, Metzner R, Kochs J, Postma JA, Pflugfelder D, Bühler J, et al. Quantitative 3d analysis of plant roots growing in soil using magnetic resonance imaging. Plant Physiol 2016;170(3):1176–88.
[59] Hillnhutter C, Sikora RA, Oerke EC, van Dusschoten D. Nuclear magnetic resonance: a tool for imaging belowground damage caused by heterodera schachtii and rhizoctonia solani on sugar beet. J Exp Bot 2011;63(1): 319–27.
[60] Rascher U, Blossfeld S, Fiorani F, Jahnke S, Jansen M, Kuhn AJ, et al. Non-invasive approaches for phenotyping of enhanced performance traits in bean. Funct Plant Biol 2011;38(12):968.
[61] Poorter H, Bühler J, van Dusschoten D, Climent J, Postma JA. Pot size matters: a meta-analysis of the effects of rooting volume on plant growth. Funct Plant Biol 2012;39(11):839.
[62] Tracy SR, Nagel KA, Postma JA, Fassbender H, Wasson A, Watt M. Crop improvement from phenotyping roots: Highlights reveal expanding opportunities. Trends Plant Sci 2020;25(1):105–18.
[63] Pierret A, Capowiez Y, Belzunces L, Moran C. 3d reconstruction and quantification of macropores using x-ray computed tomography and image analysis. Geoderma 2002;106(3–4):247–71.
[64] Flavel RJ, Guppy CN, Tighe M, Watt M, McNeill A, Young IM. Non-destructive quantification of cereal roots in soil using high-resolution x-ray tomography. J Exp Bot 2012;63 (7):2503–11.
[65] Gargiulo L, Grimberg Đ, Repo-Carrasco-Valencia R, Carlsson AS, Mele G. Morpho-densitometric traits for quinoa (chenopodium quinoa willd.) seed phenotyping by two x-ray micro-CT scanning approaches. J Cereal Sci 2019;90:102829.
[66] Hughes N, Askew K, Scotson CP, Williams K, Sauze C, Corke F, et al. Non-destructive, high-content analysis of wheat grain traits using x-ray micro computed tomography. Plant Methods 2017;13(1).
[67] Soltaninejad M, Sturrock CJ, Griffiths M, Pridmore TP, Pound MP. Three dimensional root ct segmentation using multi-resolution encoder-decoder networks. IEEE Trans Image Process 2020;29:6667–79.
[68] Metzner R, Eggert A, van Dusschoten D, Pflugfelder D, Gerth S, Schurr U, et al. Direct comparison of MRI and x-ray CT technologies for 3d imaging of root systems in soil: potential and challenges for root trait quantification. Plant Methods 2015;11(1):17.
[69] Grand-Brochier M, Vacavant A, Cerutti G, Kurtz C, Weber J, Tougne L. Tree leaves extraction in natural images: Comparative study of preprocessing tools and segmentation methods. IEEE Trans Image Process 2015;24(5):1549–60.
[70] Lee U, Chang S, Putra GA, Kim H, Kim DH. An automated, high-throughput plant phenotyping system using machine learning-based plant segmentation and image analysis. PLOS ONE 2018;13(4):e0196615.
[71] Mochida K, Koda S, Inoue K, Hirayama T, Tanaka S, Nishii R, et al. Computer vision-based phenotyping for improvement of plant productivity: a machine learning perspective. GigaScience 2018;8(1).
[72] Guerrero J, Pajares G, Montalvo M, Romeo J, Guijarro M. Support vector machines for crop/weeds identification in maize fields. Expert Syst Appl 2012;39(12):11149–55.
[73] Choudhury SD, Bashyam S, Qiu Y, Samal A, Awada T. Holistic and component plant phenotyping using temporal image sequence. Plant Methods 2018;14(1).
[74] Lima M, Krus A, Valero C, Barrientos A, Cerro J, Roldn Gmez J. Monitoring plant status and fertilization strategy through multispectral images. Sensors 2020;20. https://doi.org/10.3390/s20020435.
[75] Meyer G, Neto JC, Jones DD, Hindman TW. Intensified fuzzy clusters for classifying plant, soil, and residue regions of interest from color images. Comput Electron Agric 2004;42 (3):161–80.
[76] Zheng L, Zhang J, Wang Q. Mean-shift-based color segmentation of images containing green vegetation. Comput Electron Agric 2009;65(1):93–8.
[77] Guo W, Rage UK, Ninomiya S. Illumination invariant segmentation of vegetation for time series wheat images based on decision tree model. Comput Electron Agric 2013;96:58–66.
[78] Woebbecke DM, Meyer GE, Bargen KV, Mortensen DA. Color indices for weed identification under various soil, residue, and lighting conditions. Trans ASAE 1995;38(1):259–69.
[79] Kataoka T, Kaneko T, Okamoto H, Hata S. Crop growth estimation system using machine vision. In: Proceedings 2003 IEEE/ASME International Conference on Advanced Intelligent Mechatronics (AIM 2003); vol. 2. IEEE; 2003. p. b1079–83.
[80] Hague T, Tillett ND, Wheeler H. Automated crop and weed monitoring in widely spaced cereals. Precision Agric 2006;7 (1):21–32.
[81] Burgos-Artizzu XP, Ribeiro A, Guijarro M, Pajares G. Real-time image processing for crop/weed discrimination in maize fields. Comput Electron Agric 2011;75(2):337–46.
[82] Reid J, Searcy S. Vision-based guidance of an agriculture tractor. IEEE Control Syst Mag 1987;7(2):39–43.
[83] Marchant JA, Tillett RD, Brivot R. Real-time segmentation of plants and weeds. Real-Time Imag 1998;4(4):243–53.
[84] Aitkenhead M, Dalgetty I, Mullins C, McDonald A, Strachan N. Weed and crop discrimination using image analysis and artificial intelligence methods. Comput Electron Agric 2003;39(3):157–71.
[85] Tellaeche A, Burgos-Artizzu XP, Pajares G, Ribeiro A. A vision-based method for weeds identification through the bayesian decision theory. Pattern Recogn 2008;41(2):521–30.
[86] Otsu N. A threshold selection method from gray-level histograms. IEEE Trans Syst Man Cybernet 1979;9(1):62–6.
[87] Gebhardt S, Kühbauch W. A new algorithm for automatic rumex obtusifolius detection in digital images using colour and texture features and the influence of image resolution. Precision Agric 2006;8(1–2):1–13.
[88] Jeon HY, Tian LF, Zhu H. Robust crop and weed segmentation under uncontrolled outdoor illumination. Sensors 2011;11 (6):6270–83.
[89] Ruiz-Ruiz G, Gómez-Gil J, Navas-Gracia L. Testing different color spaces based on hue for the environmentally adaptive segmentation algorithm (EASA). Comput Electron Agric 2009;68(1):88–96.
[90] Zheng L, Shi D, Zhang J. Segmentation of green vegetation of crop canopy images based on mean shift and fisher linear discriminant. Pattern Recogn Lett 2010;31(9):920–5.
[91] Bai X, Cao Z, Wang Y, Yu Z, Hu Z, Zhang X, et al. Vegetation segmentation robust to illumination variations based on clustering and morphology modelling. Biosyst Eng 2014;125:80–97.
[92] Pape JM, Klukas C. 3-d histogram-based segmentation and leaf detection for rosette plants. In: Computer Vision - ECCV 2014 Workshops. Springer International Publishing; 2015. p. 61–74.
[93] Scharr H, Minervini M, Fischbach A, Tsaftaris SA. Annotated image datasets of rosette plants. Technical Report No FZJ-2014-03837; 2014.
[94] Minervini M, Fischbach A, Scharr H, Tsaftaris S. Plant phenotyping datasets; 2015. http://www.plant-phenotyping.org/datasets.

Please cite this article as: S. Kolhar and J. Jagtap, Plant trait estimation and classification studies in plant phenotyping using machine vision – A review, Information Processing in Agriculture, https://doi.org/10.1016/j.inpa.2021.02.006

[95] Wang Z, Wang K, Yang F, Pan S, Han Y. Image segmentation of overlapping leaves based on chan–vese model and sobel operator. Inform Process Agric 2018;5(1):1–10.
[96] Tsaftaris SA, Minervini M, Scharr H. Machine learning for plant phenotyping needs image processing. Trends Plant Sci 2016;21(12):989–91.
[97] Minervini M, Abdelsamea MM, Tsaftaris SA. Image-based plant phenotyping with incremental learning and active contours. Ecol Informat 2014;23:35–48.
[98] Al-Shakarji NM, Kassim YM, Palaniappan K. Unsupervised learning method for plant and leaf segmentation. In: 2017 IEEE Applied Imagery Pattern Recognition Workshop (AIPR). IEEE; 2017. p. 1–4.
[99] Bodner G, Nakhforoosh A, Arnold T, Leitner D. Hyperspectral imaging: a novel approach for plant root phenotyping. Plant Methods 2018;14(1).
[100] Jiang, Wang, Zhuang, Li, Li, Gong. Leaf counting with multi-scale convolutional neural network features and fisher vector coding. Symmetry 2019;11(4):516.
[101] Falk KG, Jubery TZ, Mirnezami SV, Parmley KA, Sarkar S, Singh A, et al. Computer vision and machine learning enabled soybean root phenotyping pipeline. Plant Methods 2020;16(1).
[102] Singh AK, Ganapathysubramanian B, Sarkar S, Singh A. Deep learning for plant stress phenotyping: Trends and future perspectives. Trends Plant Sci 2018;23(10):883–98.
[103] Aich S, Stavness I. Leaf counting with deep convolutional and deconvolutional networks. In: 2017 IEEE International Conference on Computer Vision Workshops (ICCVW). IEEE; 2017. p. 2080–9.
[104] Pound MP, Atkinson JA, Townsend AJ, Wilson MH, Griffiths M, Jackson AS, et al. Deep machine learning provides state-of-the-art performance in image-based plant phenotyping. GigaScience 2017;6(10).
[105] Salvador A, Bellver M, Baradad M, Marqués F, Torres J, i Nieto XG. Recurrent neural networks for semantic instance segmentation. ArXiv 2017;abs/1712.00617.
[106] Dobrescu A, Giuffrida MV, Tsaftaris SA. Leveraging multiple datasets for deep leaf counting. In: 2017 IEEE International Conference on Computer Vision Workshops (ICCVW). IEEE; 2017. p. 2072–9.
[107] Russakovsky O, Deng J, Su H, Krause J, Satheesh S, Ma S, et al. ImageNet large scale visual recognition challenge. Int J Comput Vision 2015;115(3):211–52.
[108] Morris D. A pyramid cnn for dense-leaves segmentation. In: 2018 15th Conference on Computer and Robot Vision (CRV); 2018. p. 238–45.
[109] Liu Y, Cen C, Che Y, Ke R, Ma Y, Ma Y. Detection of maize tassels from UAV RGB imagery with faster r-CNN. Remote Sens 2020;12(2):338.
[110] Kumar JP, Domnic S. Rosette plant segmentation with leaf count using orthogonal transform and deep convolutional neural network. Mach Vis Appl 2020;31(1–2).
[111] Lin Z, Guo W. Sorghum panicle detection and counting using unmanned aerial system images and deep learning. Front Plant Sci 2020;11:1346.
[112] Ma J, Li X, Wen H, Fu Z, Zhang L. A key frame extraction method for processing greenhouse vegetables production monitoring video. Comput Electron Agric 2015;111:92–102.
[113] Lu H, Cao Z, Xiao Y, Zhuang B, Shen C. TasselNet: counting maize tassels in the wild via local counts regression network. Plant Methods 2017;13(1).
[114] Pandey P, Ge Y, Stoerger V, Schnable JC. High throughput in vivo analysis of plant leaf chemical properties using hyperspectral imaging. Front Plant Sci 2017;8.
[115] Chinnusamy V, Misra T, Kumar S, Sahoo R, Raju D. Artificial neural network for estimating leaf fresh weight of rice plant through visual-nir imaging. Indian J Agric Sci 2019;89:1698–702.
[116] Rehman TU, Ma D, Wang L, Zhang L, Jin J. Predictive spectral analysis using an end-to-end deep model from hyperspectral images for high-throughput plant phenotyping. Comput Electron Agric 2020;177:105713.
[117] Das Choudhury S, Goswami S, Bashyam S, Samal A, Awada T. Automated stem angle determination for temporal plant phenotyping analysis. In: Proceedings of the IEEE International Conference on Computer Vision Workshops. p. 2022–9.
[118] Agarwal B. Detection of plant emergence based on spatio temporal image sequence analysis; 2017.
[119] Jiang Y, Li C, Xu R, Sun S, Robertson JS, Paterson AH. Deepflower: a deep learning-based approach to characterize flowering patterns of cotton plants in the field. Plant Methods 2020;16(1):1–17.
[120] Vandenberghe B, Depuydt S, Messem AV. How to make sense of 3d representations for plant phenotyping: a compendium of processing and analysis techniques; 2018.
[121] Aksoy EE, Abramov A, Wörgötter F, Scharr H, Fischbach A, Dellen B. Modeling leaf growth of rosette plants using infrared stereo image sequences. Comput Electron Agric 2015;110:78–90.
[122] He J, Harrison R, Li B. A novel 3d imaging system for strawberry phenotyping. Plant Methods 2017;13.
[123] Bernotas G, Scorza LCT, Hansen MF, Hales IJ, Halliday KJ, Smith LN, et al. A photometric stereo-based 3d imaging system using computer vision and deep learning for tracking plant growth. GigaScience 2019;8(5).
[124] Hu W, Zhang C, Jiang Y, Huang C, Liu Q, Xiong L, et al. Nondestructive 3d image analysis pipeline to extract rice grain traits using x-ray computed tomography. Plant Phenomics 2020;2020:1–12.
[125] Choudhury SD, Maturu S, Samal A, Stoerger V, Awada T. Leveraging image analysis to compute 3d plant phenotypes based on voxel-grid plant reconstruction. Front Plant Sci 2020;11.
[126] Lee SH, Chang YL, Chan CS, Remagnino P. Plant identification system based on a convolutional neural network for the lifeclef 2016 plant classification task. In: CLEF; 2016. p. 502–10.
[127] Joly A, Goau H, Glotin H, Spampinato C, Bonnet P, Vellinga WP, et al. LifeCLEF 2016: Multimedia life species identification challenges. In: Lecture Notes in Computer Science. Springer International Publishing; 2016. p. 286–310.
[128] Lottes P, Hörferlin M, Sander S, Stachniss C. Effective vision-based classification for separating sugar beets and weeds for precision farming. J Field Robot 2016;34(6):1160–78.
[129] Lee SH, Chan CS, Mayo SJ, Remagnino P. How deep learning extracts and learns leaf features for plant classification. Pattern Recogn 2017;71:1–13.
[130] Guo D, Juan J, Chang L, Zhang J, Huang D. Discrimination of plant root zone water status in greenhouse production based on phenotyping and machine learning techniques. Sci Rep 2017;7(1).
[131] Namin ST, Esmaeilzadeh M, Najafi M, Brown TB, Borevitz JO. Deep phenotyping: deep learning for temporal phenotype/genotype classification. Plant Methods 2018;14(1).
[132] Beikmohammadi A, Faez K. Leaf classification for plant recognition with deep transfer learning. In: 2018 4th Iranian Conference on Signal Processing and Intelligent Systems (ICSPIS). IEEE; 2018. p. 21–6.
[133] Wu SG, Bao FS, Xu EY, Wang Y, Chang Y, Xiang Q. A leaf recognition algorithm for plant classification using probabilistic neural network. In: 2007 IEEE International Symposium on Signal Processing and Information Technology. p. 11–6.
[134] Kumar N, Belhumeur PN, Biswas A, Jacobs DW, Kress WJ, Lopez IC, et al. Leafsnap: A computer vision system for

Please cite this article as: S. Kolhar and J. Jagtap, Plant trait estimation and classification studies in plant phenotyping using machine vision – A review, Information Processing in Agriculture, https://doi.org/10.1016/j.inpa.2021.02.006

automatic plant species identification. In: Computer Vision – ECCV 2012. Berlin Heidelberg: Springer; 2012. p. 502–16.
[135] Moghimi A, Yang C, Marchetto PM. Ensemble feature selection for plant phenotyping: A journey from hyperspectral to multispectral imaging. IEEE Access 2018;6:56870–84.
[136] Venal MCA, Fajardo AC, Hernandez AA. Plant stress classification for smart agriculture utilizing convolutional neural network - support vector machine. In: 2019 International Conference on ICT for Smart Society (ICISS). IEEE; 2019. p. 1–5.
[137] Pacifico LD, Britto LF, Oliveira EG, Ludermir TB. Automatic classification of medicinal plant species based on color and texture features. In: 2019 8th Brazilian Conference on Intelligent Systems (BRACIS). IEEE; 2019. p. 741–6.
[138] Fuentes-Pacheco J, Torres-Olivares J, Roman-Rangel E, Cervantes S, Juarez-Lopez P, Hermosillo-Valadez J, et al. Fig plant segmentation from aerial images using a deep convolutional encoder-decoder network. Remote Sens 2019;11(10):1157.
[139] Anami BS, Malvade NN, Palaiah S. Classification of yield affecting biotic and abiotic paddy crop stresses using field images. Inform Process Agric 2020;7(2):272–85.
[140] Ghosal S, Blystone D, Singh AK, Ganapathysubramanian B, Singh A, Sarkar S. An explainable deep machine vision framework for plant stress phenotyping. Proc Nat Acad Sci 2018;115(18):4613–8.
[141] Krajewski P, Chen D, Ćwiek H, van Dijk AD, Fiorani F, Kersey P, et al. Towards recommendations for metadata and data handling in plant phenotyping. J Exp Bot 2015;66 (18):5417–27.
[142] Lobet G. Image analysis in plant sciences: Publish then perish. Trends Plant Sci 2017;22.
[143] Cruz J, Yin X, Liu X, Imran S, Morris D, Kramer D, et al. Multi-modality imagery database for plant phenotyping. Mach Vis Appl 2016;7:1–15.
[144] Uchiyama H, Sakurai S, Mishima M, Arita D, Okayasu T, Shimada A, et al. An easy-to-setup 3d phenotyping platform for komatsuna dataset. In: 2017 IEEE International Conference on Computer Vision Workshops (ICCVW). p. 2038–45.

Shrikrishna Kolhar received the B.E. degree in Electronics and Telecommunication Engineering at Savitribai Phule Pune University, Pune, India. He received the M.E. degree in Electronics - Digital Systems at Savitribai Phule Pune University, Pune, India. He is working towards the PhD degree at Symbiosis International (Deemed University), Pune, India. He is presently working as an Assistant Professor in Vidya Pratishthan's Kamalnayan Bajaj Institute of Engineering and Technology, Baramati, India. His areas of interest include digital image processing, computer vision, machine learning and deep learning.

Jayant Jagtap received the B.E. degree in Electronics and Telecommunication Engineering at Dr. Babasaheb Ambedkar Marathwada University, Aurangabad, India. He received the M. Tech. degree in Electronics as well as PhD degree in Electronics and Telecommunication Engineering at Swami Ramanand Teerth Marathwada University, Nanded, India. He is presently working as an Assistant Professor in Symbiosis Institute of Technology, Symbiosis International (Deemed University), Pune, India. His areas of interest include digital image processing, medical image processing, pattern recognition, computer vision, machine learning and deep learning.

Please cite this article as: S. Kolhar and J. Jagtap, Plant trait estimation and classification studies in plant phenotyping using machine vision – A review, Information Processing in Agriculture, https://doi.org/10.1016/j.inpa.2021.02.006